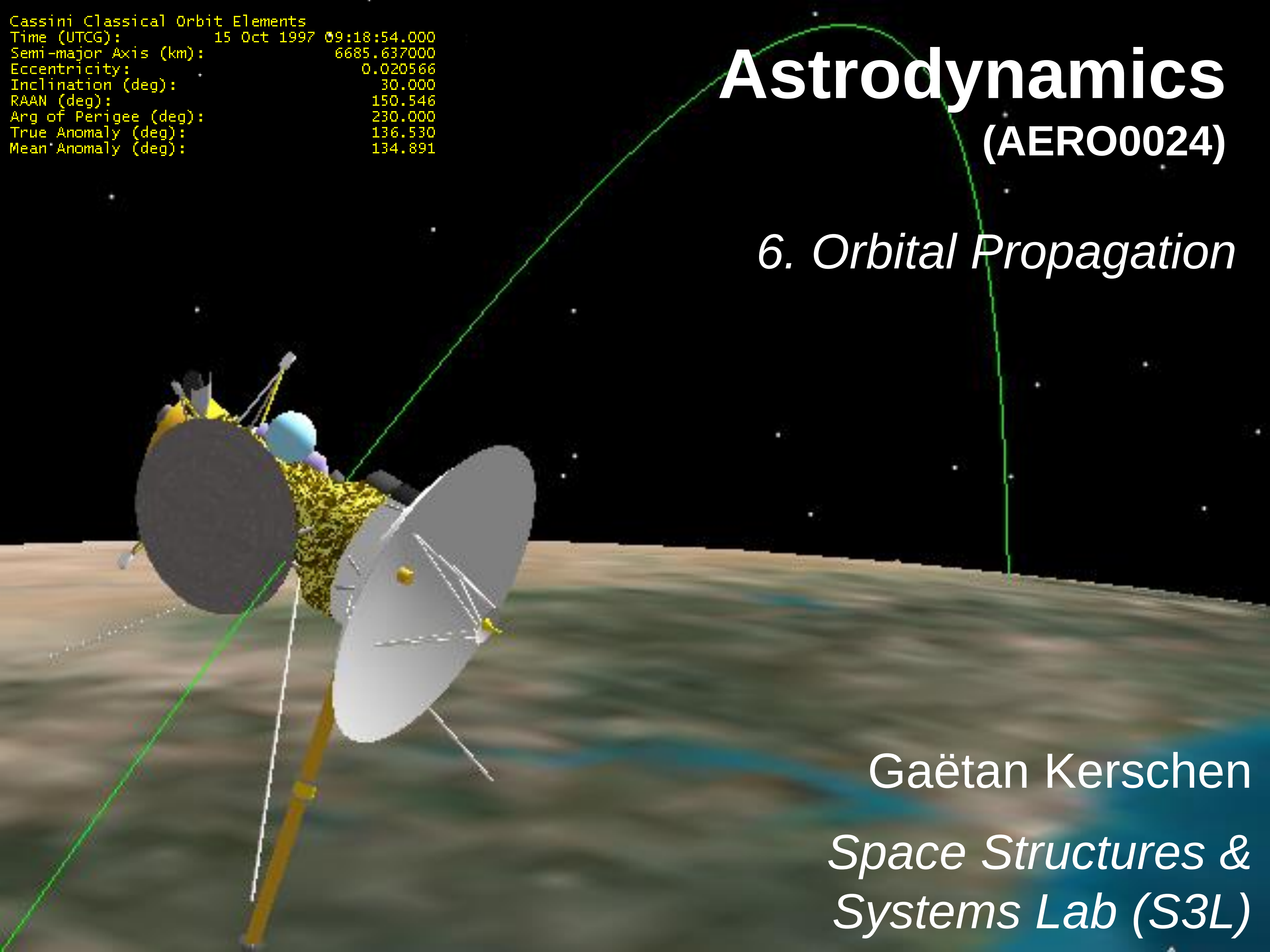

Astrodynamics
(AERO0024)

6. Orbital Propagation

Gaëtan Kerschen

Space Structures & Systems Lab (S3L)

Two-body problem

Dominant perturbations

Orbital elements
$(a, e, i, \Omega, \omega)$ are constant

Real satellites may undergo perturbations

This lecture:

1. Effects of these perturbations on the orbital elements ?

2. Computation of these effects ?

Why different propagators ?

Analytic propagation:

Better understanding of the perturbing forces.

Useful for mission planning (fast answer): e.g., lifetime computation.

Numerical propagation:

The high accuracy required today for satellite orbits can only be achieved by using numerical integration.

Incorporation of any arbitrary disturbing acceleration (versatile).

Orbital propagation

$$\dot{\Omega} = \sqrt{\frac{a(1-e^2)}{\mu}}\,\frac{N\sin\theta_2}{\sin i\left(1+e\cos\theta\right)}$$

Analytic treatment

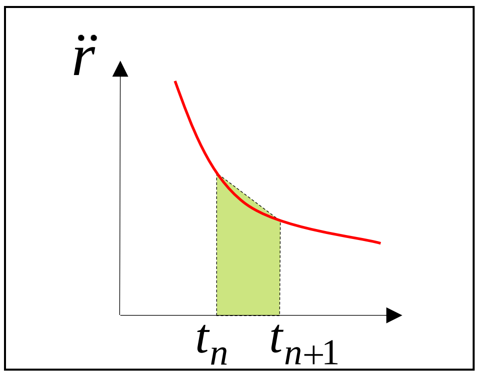

Numerical methods

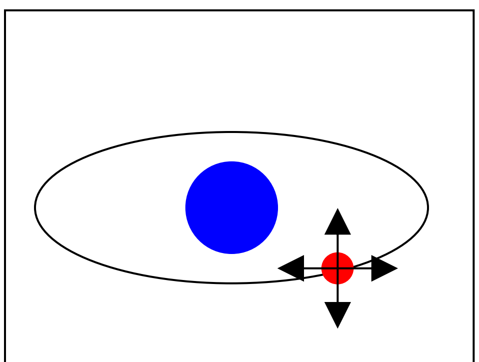

ISS and geostationary satellites

Analytic treatment: definition

Position and velocity at a requested time are computed directly from initial conditions in a single step.

Analytic propagators use a closed-form solution of the time-dependent motion of a satellite.

Mainly used for the two dominant perturbations, drag and earth oblateness.

Analytic treatment: pros and cons

Useful for mission planning and analysis (fast and insight):

Though the numerical integration methods can generate more accurate ephemeris of a satellite with respect to a complex force model, the analytical solutions represent a manifold of solutions for a large domain of initial conditions and parameters.

But less accurate than numerical integration.

Be aware of the assumptions made !

A motivating example: ISS 2-body

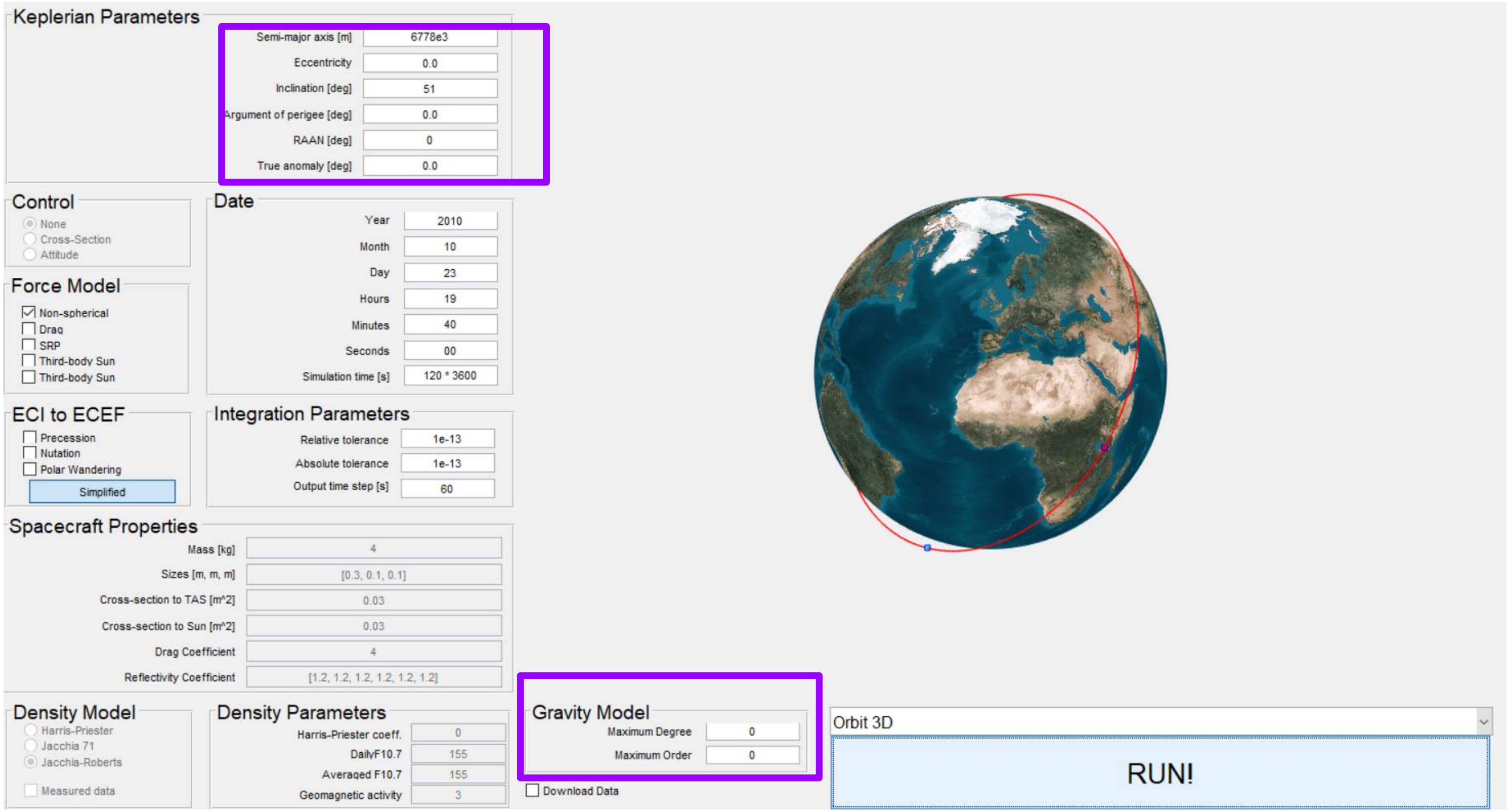

A motivating example: ISS J2

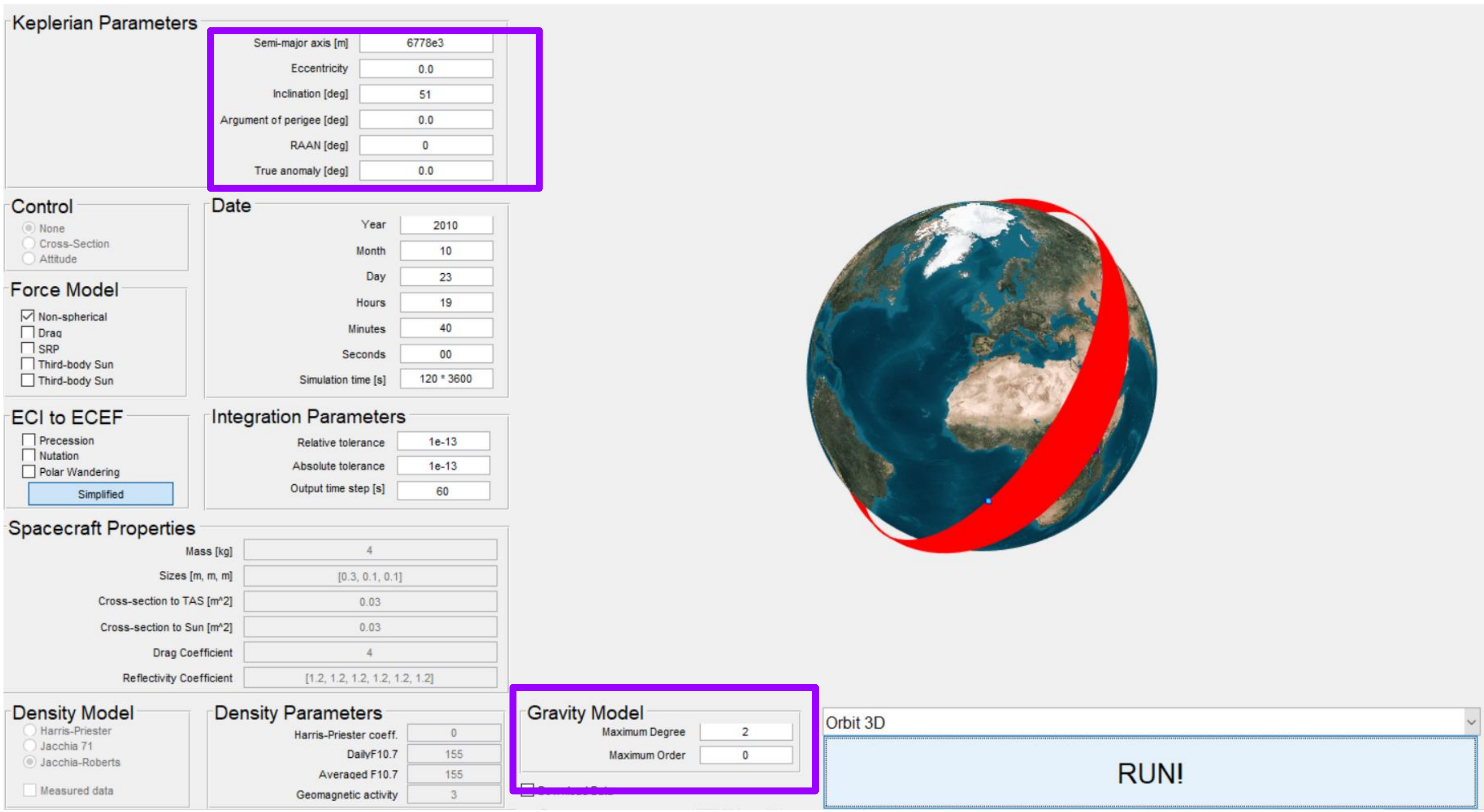

Can we predict the RAAN drift due to J2 analytically ?

Disturbing acceleration (specific force)

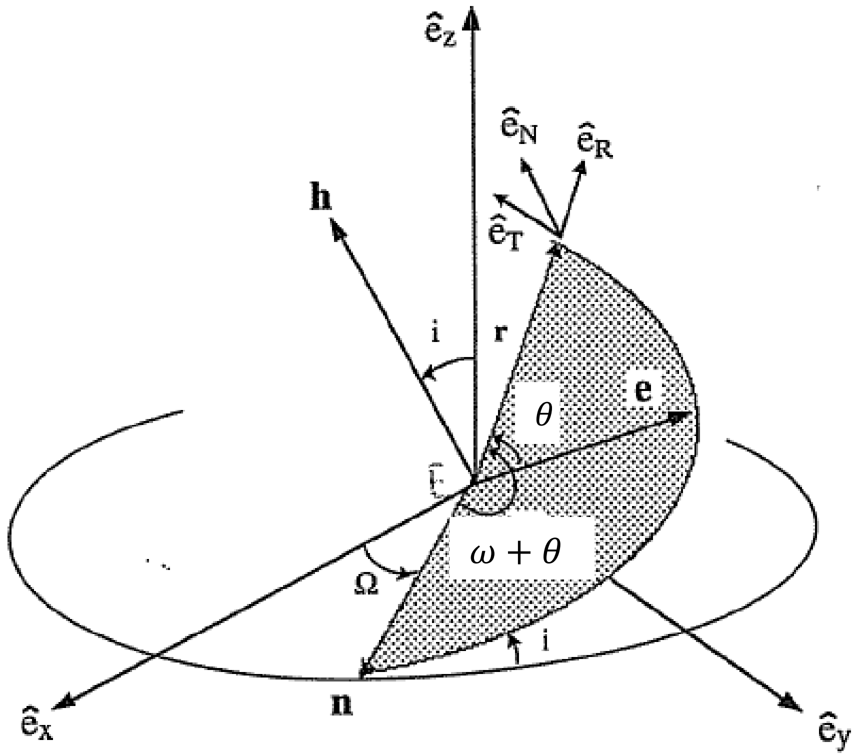

$$\mathbf{r} = r\ \hat{\boldsymbol{e}}_R$$

$$\dot{\mathbf{r}} = \dot{r}\hat{\mathbf{e}}_R + r\dot{\theta}\hat{\mathbf{e}}_T$$

(assuming small variations of ω !)

$$\mathbf{a}_{perturbed} = \mathbf{F} = R\hat{\boldsymbol{e}}_R + T\hat{\mathbf{e}}_T + N\hat{\mathbf{e}}_N$$

Rotating basis whose origin is fixed to the satellite

Variation of parameters (VOP)

Originally developed by Euler and improved by Lagrange (conservative) and Gauss (nonconservative).

It is called variation of parameters, because the orbital elements (i.e., the constant parameters in the two-body equations) are changing in the presence of perturbations. The energy and the angular momentum are no longer constant either.

The VOP equations are a system of first-order ODEs that describe the rates of change of the orbital elements.

$$\boxed{\dot{a}, \dot{i}, \dot{e}, \dot{\Omega}, \dot{\omega}, \dot{M} \ ?}$$

End result: perturbation equations (Gauss)

$$\dot{\Omega} = \sqrt{\frac{a(1-e^2)}{\mu}} \frac{N \sin(\omega+\theta)}{\sin i\,(1+e\cos\theta)}$$

$$\dot{a} = 2\sqrt{\frac{a^3}{\mu\left(1-e^2\right)}}\left[R e \sin\theta + T\left(1+e\cos\theta\right)\right]$$

$$\dot{i} = \sqrt{\frac{a(1-e^2)}{\mu}} \frac{N \cos(\omega+\theta)}{(1+e\cos\theta)}$$

$$\dot{e} = \sqrt{\frac{a(1-e^2)}{\mu}}\left[R\sin\theta + T\left(\cos\theta+\cos E\right)\right]$$

$$\dot{\omega} = -\dot{\Omega}\cos i + \frac{1}{e}\sqrt{\frac{a(1-e^2)}{\mu}}\left[-R\cos\theta + \frac{T\sin\theta\left(2+e\cos\theta\right)}{1+e\cos\theta}\right]$$

$$M = nt - \chi, \text{with } \dot{\chi} = \sqrt{\frac{a}{\mu}}\frac{(1-e^2)\left[R\left(2e-\cos\theta-e\cos^2\theta\right)+T\sin\theta\left(2+e\cos\theta\right)\right]}{e\left(1+e\cos\theta\right)}$$

J.E. Prussing, B.A. Conway, *Orbital Mechanics*, Oxford University Press

Objective: Express the derivatives of the parameters as a function of the parameters themselves and the forces R, T and N.

Let's demonstrate da/dt (energy variation)

Energy of a satellite in elliptical orbit

$$\varepsilon = \frac{-\mu}{2a} \longrightarrow \dot{\varepsilon} = \frac{\mu}{2a^2}\dot{a} \longrightarrow \dot{a} = \frac{2a^2}{\mu}\dot{\varepsilon}$$

Time rate-of-change of the work done by the disturbing force (power)

$$\dot{\varepsilon} = \mathbf{F}\dot{\mathbf{r}} = \mathbf{F}\left(\dot{r}\hat{\mathbf{e}}_R + r\dot{\theta}\hat{\mathbf{e}}_T\right) = \dot{r}R + r\dot{\theta}T$$

2-body

$$\dot{\theta} = \frac{h}{r^2}$$

$$r = \frac{h^2}{\mu}\frac{1}{(1 + e\cos\theta)} \longrightarrow \frac{dr}{d\theta} = \frac{h^2}{\mu}\frac{e\sin\theta}{(1 + e\cos\theta)^2}$$

$$\Rightarrow \quad \dot{r} = \frac{dr}{d\theta}\dot{\theta} = \frac{h^2}{\mu}\frac{e\sin\theta}{(1 + e\cos\theta)^2}\frac{h}{r^2} = \frac{h^2}{\mu}e\sin\theta\frac{\mu^2 r^2}{h^4}\frac{h}{r^2} = \frac{e\mu}{h}\sin\theta$$

$$\Rightarrow \quad \dot{a} = \frac{2a^2}{\mu}\left(\frac{e\mu\sin\theta}{h}R + \frac{h}{r}T\right)$$

$$r = \frac{h^2}{\mu}\frac{1}{(1 + e\cos\theta)}$$

$Simplify$

The variation of *a* vs. the perturbing force

$$\dot{a} = \frac{2a^2}{\mu}\left(\frac{\mu e \sin\theta}{h}R + \frac{h}{r}T\right) = \frac{2a^2}{h}\left(e\sin\theta\, R + \frac{h^2}{\mu r}T\right)$$

$$= \frac{2a^2}{h}\big(Re\sin\theta + T(1 + e\cos\theta)\big)$$

$$r = \frac{h^2}{\mu}\frac{1}{(1 + e\cos\theta)}$$

2-body: $h = \sqrt{\mu a(1 - e^2)}$

$$\dot{a} = 2\sqrt{\frac{a^3}{\mu(1 - e^2)}}\big(Re\sin\theta + T(1 + e\cos\theta)\big)$$

Let's demonstrate de/dt (momentum variation)

Rotational motion 2nd law:

$$\dot{\boldsymbol{h}} = \boldsymbol{r} \times \boldsymbol{F} = (r,0,0) \times (R,T,N) = rT\hat{\boldsymbol{e}}_N - rN\hat{\boldsymbol{e}}_T$$

$\hat{\boldsymbol{e}}_T$ always normal to **h**, so only
$\hat{\boldsymbol{e}}_N$ changes the magnitude of **h**

$\Rightarrow$ $\dot{h} = rT$ with $h = \sqrt{\mu a(1-e^2)}$

$$e = \sqrt{1 - \frac{h^2}{\mu a}} \longrightarrow \dot{e} = \frac{1}{2}\left(1 - \frac{h^2}{\mu a}\right)^{-1/2}\left[\frac{-2h}{\mu a}\frac{dh}{dt} + \frac{h^2}{\mu a^2}\frac{da}{dt}\right]$$

$h = \sqrt{\mu a(1-e^2)}$

$$\dot{e} = \frac{1}{2}\left(\frac{\mu a - \mu a(1-e^2)}{\mu a}\right)^{-1/2}\left[\frac{-2h}{\mu a}\frac{dh}{dt} + \frac{h^2}{\mu a^2}\frac{da}{dt}\right]$$

Simplify

$$\dot{e} = \frac{1}{2e}\left[\frac{-2h}{\mu a}\frac{dh}{dt} + \frac{h^2}{\mu a^2}\frac{da}{dt}\right]$$

$$\Rightarrow \dot{e} = \frac{1}{2e}\left[\frac{-2h}{\mu a}rT + \frac{2h^2}{\mu a^2}\sqrt{\frac{a^3}{\mu(1-e^2)}}\big(Re\sin\theta + T(1 + e\cos\theta)\big)\right]$$

Let's demonstrate de/dt (momentum variation)

$$\dot{e} = \frac{1}{2e}\left[\frac{-2h}{\mu a}rT + \frac{2h^2}{\mu a^2}\sqrt{\frac{a^3}{\mu(1-e^2)}}\big(Re\sin\theta + T(1+e\cos\theta)\big)\right]$$

$h = \sqrt{\mu a(1-e^2)}$

$$= \frac{-h}{\mu ae}rT + \frac{\mu a(1-e^2)}{\mu e\sqrt{a}}\sqrt{\frac{1}{\mu(1-e^2)}}\big(Re\sin\theta + T(1+e\cos\theta)\big)$$

Simplify

$$= \frac{-h}{\mu ae}rT + \frac{1}{e}\sqrt{\frac{a(1-e^2)}{\mu}}\big(Re\sin\theta + T(1+e\cos\theta)\big)$$

Factorize T

$$= \sqrt{\frac{a(1-e^2)}{\mu}}R\sin\theta + T\left(\frac{-h}{\mu ae}r + \frac{1}{e}\sqrt{\frac{a(1-e^2)}{\mu}}(1+e\cos\theta)\right)$$

Distribute

$$= \sqrt{\frac{a(1-e^2)}{\mu}}R\sin\theta + T\left(\sqrt{\frac{a(1-e^2)}{\mu}}\cos\theta + \frac{-h}{\mu ae}r + \frac{1}{e}\sqrt{\frac{a(1-e^2)}{\mu}}\right)$$

Let’s demonstrate de/dt (momentum variation)

$$\dot{e} = \sqrt{\frac{a(1-e^2)}{\mu}} R \sin\theta + T\left(\sqrt{\frac{a(1-e^2)}{\mu}} \cos\theta + \frac{-h}{\mu a e} r + \frac{1}{e}\sqrt{\frac{a(1-e^2)}{\mu}}\right)$$

$$= \sqrt{\frac{a(1-e^2)}{\mu}} (R \sin\theta + T\cos\theta) + T\left(\frac{-h}{\mu a e} r + \frac{1}{e}\sqrt{\frac{a(1-e^2)}{\mu}}\right)$$

$$r = (1 - ecosE)a$$

$$= \frac{-h}{\mu a e}(1 - ecosE)a + \frac{1}{e}\sqrt{\frac{a(1-e^2)}{\mu}}$$

$$h = \sqrt{\mu a(1-e^2)}$$

$$= \frac{-1}{e}\sqrt{\frac{a(1-e^2)}{\mu}}(1 - ecosE) + \frac{1}{e}\sqrt{\frac{a(1-e^2)}{\mu}}$$

Simplify

$$= \sqrt{\frac{a(1-e^2)}{\mu}} cosE$$

r as a function of the eccentric anomaly E

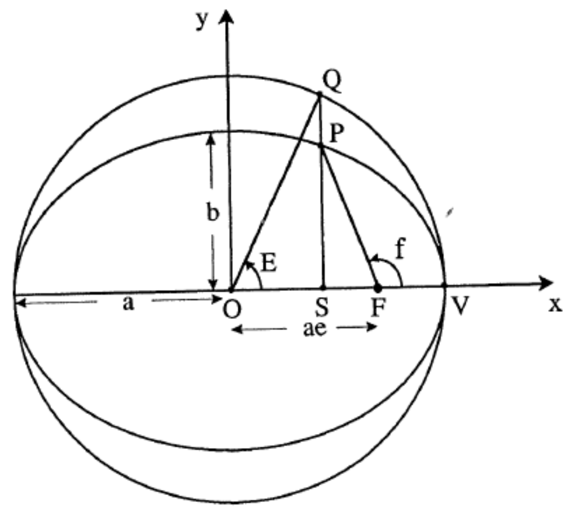

Fig. 2.1 Definition of Eccentric Anomaly

passage. The value of τ represents the *sixth* independent constant, in addition to the vectors **h** and **e**, needed for a unique solution to the two-body problem, as discussed in Sec. 1.4. As a consequence of Kepler's second law, the mean anomaly will lag behind the true anomaly in the first and second quadrants. The situation will then reverse in the third and fourth quadrants. As shown in Prob. 2.4 the mean and eccentric anomalies exhibit the same property.

Unfortunately, Eq. (2.7) still does not provide position, f, as a function of t. We need to relate true anomaly f to eccentric anomaly E. With reference again to Fig. 2.1, we see that the length of line segment OS is

$$OS = a \cos E = ae + r \cos f$$

or, employing Eq. (1.33) for r yields

$$a \cos E = ae + \frac{a(1-e^2)\cos f}{1 + e \cos f} \qquad (2.8)$$

or

$$\cos E = \frac{e + \cos f}{1 + e \cos f} \qquad (2.9)$$

Utilizing Eq. (2.9)

$$\tan^2 \frac{E}{2} = \frac{1 - \cos E}{1 + \cos E} = \left(\frac{1-e}{1+e}\right)\left(\frac{1 - \cos f}{1 + \cos f}\right) \qquad (2.10)$$

which yields

$$\tan \frac{E}{2} = \left(\frac{1-e}{1+e}\right)^{1/2} \tan \frac{f}{2} \qquad (2.11)$$

Equation (2.11) is a very convenient conversion formula that alleviates quadrant ambiguity (see Prob. 2.1). It also follows directly from Eq. (2.9) that

$$r = \frac{a(1-e^2)}{1 + e \cos f} = a(1 - e \cos E) \qquad (2.12)$$

which describes the radius directly in terms of eccentric anomaly.

Kepler's Eq. (2.7) has many applications in orbital mechanics that fall into two cases: (1) For a given elliptic orbit, determine the time at which the orbiting body will be at a specified position in the orbit, and (2) determine the position of the orbiting body at a specified time. These two cases sound similar, but are quite different both in terms of the physical problems they represent and the degree of difficulty in solving Kepler's equation.

In Case 1, the solution to Eq. (2.7) is straightforward. The value of E corresponding to the specified position in the orbit is calculated, such as by using Eq. (2.11). The time is then calculated directly from Eq. (2.7). An application of this case is the determination of the time at which an earth satellite passes from sunlight into the earth's shadow. The location of this point is known from the geometry. The time at which the satellite passes into and out of the earth's shadow determines the amount of time during each orbit electrical power must be drawn from batteries and the amount of time solar cells can recharge the batteries.

In Case 2 on the other hand, the solution of Kepler's equation is much more difficult because the equation is transcendental in the unknown variable E. One cannot write a closed-form expression for E as a function of the time t, although many famous mathematicians have tried over the years. However, there are important situations in which the location of a satellite at a particular time must be known. Examples include sending and receiving radio signals and performing a rendezvous with an orbiting space station. There are various approximations and series expansion methods that can be used, but numerical iteration, as discussed in the next section, is commonly employed to obtain a solution.

When one is faced with solving a transcendental equation, the questions of existence and uniqueness of a solution must be addressed. It would be silly to attempt to iteratively determine a real-valued solution to an

The variation of *e* vs. the perturbing force

$$= \sqrt{\frac{a(1-e^2)}{\mu}}(R\sin\theta + T\cos\theta) + T\sqrt{\frac{a(1-e^2)}{\mu}}cosE$$

$$\Downarrow$$

$$\dot{e} = \sqrt{\frac{a(1-e^2)}{\mu}}\big(R\sin\theta + T(\cos\theta + cosE)\big)$$

Perturbation equations (Gauss)

Can we predict the RAAN drift due to J2 analytically ?

$$\dot{\Omega} = \sqrt{\frac{a(1-e^2)}{\mu}} \frac{N \sin(\omega+\theta)}{\sin i\,(1+e\cos\theta)}$$

$$\dot{a} = 2\sqrt{\frac{a^3}{\mu\left(1-e^2\right)}}\left[\mathrm{R}\sin\theta + T\left(1+e\cos\theta\right)\right]$$

$$\dot{i} = \sqrt{\frac{a(1-e^2)}{\mu}} \frac{N \cos(\omega+\theta)}{(1+e\cos\theta)}$$

$$\dot{e} = \sqrt{\frac{a(1-e^2)}{\mu}}\left[R\sin\theta + T\left(\cos\theta+\cos E\right)\right]$$

$$\dot{\omega} = -\dot{\Omega}\cos i + \frac{1}{e}\sqrt{\frac{a(1-e^2)}{\mu}}\left[-R\cos\theta + \frac{T\sin\theta\left(2+e\cos\theta\right)}{1+e\cos\theta}\right]$$

$$M = nt - \chi, \text{with } \dot{\chi} = \sqrt{\frac{a}{\mu}}\frac{(1-e^2)\left[R\left(2e-\cos\theta-e\cos^2\theta\right)+T\sin\theta\left(2+e\cos\theta\right)\right]}{e\left(1+e\cos\theta\right)}$$

J.E. Prussing, B.A. Conway, *Orbital Mechanics*, Oxford University Press

Can we predict the J2-drift in longitude ?

$$U_{J_2} = \frac{-\mu}{2r}\left(\frac{R_\oplus}{r}\right)^2 J_2\left(\frac{3z^2}{r^2} - 1\right) \Rightarrow N = \frac{-3\mu J_2 {R_\oplus}^2}{r^4} \sin i \sin(\omega + \theta) \cos i$$

Exercise: prove it !

$$\dot{\Omega} = -3J_2{R_\oplus}^2\sqrt{\frac{a(1-e^2)}{\mu}}\frac{\mu}{r^4}\frac{(\sin(\omega+\theta))^2\cos i}{(1+e\cos\theta)}$$

$$r = \frac{h^2}{\mu}\frac{1}{(1+e\cos\theta)}$$

$$= -3J_2{R_\oplus}^2\sqrt{\frac{a(1-e^2)}{\mu}}\frac{\mu^5}{h^8}(\sin(\omega+\theta))^2\cos i(1+e\cos\theta)^3$$

$$h = \sqrt{\mu a(1-e^2)}$$

$$= -3J_2{R_\oplus}^2\sqrt{\frac{a(1-e^2)}{\mu}}\frac{\mu^5}{(\mu a(1-e^2))^4}(\sin(\omega+\theta))^2\cos i(1+e\cos\theta)^3$$

$Simplify$

$$= -3J_2{R_\oplus}^2\frac{\sqrt{\mu}}{(a(1-e^2))^{7/2}}(\sin(\omega+\theta))^2\cos i(1+e\cos\theta)^3$$

$$= -3J_2{R_\oplus}^2\frac{\sqrt{\mu}}{(a(1-e^2))^{7/2}}(\sin\beta)^2\cos i(1+e\cos(\beta-\omega))^3$$

$$\beta = \omega + \theta = argument\ of\ latitude$$

Can we predict the J2-drift in longitude ?

$$\dot{\Omega} = \frac{d\Omega}{d\beta}\frac{d\beta}{dt} \cong \frac{d\Omega}{d\beta}\;\frac{h}{r^2}$$

$$\frac{d\Omega}{d\beta} = \frac{-3J_2{R_\oplus}^2}{(a(1-e^2))^2}\,(\sin\beta)^2\cos i(1+e\cos(\beta-\omega))$$

We average over one orbit

$$\frac{d\Omega}{d\beta}_{AVG} = \frac{-3J_2{R_\oplus}^2}{(a(1-e^2))^2}\cos i\,\frac{1}{2\pi}\int_0^{2\pi}(\sin\beta)^2\;(1+e\cos(\beta-\omega))\,d\beta$$

$$= \frac{1}{2\pi}\int_0^{2\pi}(\sin\beta)^2\;(1+e\cos\beta\cos\omega+e\sin\beta\sin\omega)\,d\beta$$

$$= \frac{1}{2\pi}\int_0^{2\pi}(\sin\beta)^2 d\beta + e\cos\omega\int_0^{2\pi}(\sin\beta)^2\cos\beta\,d\beta + e\sin\omega\int_0^{2\pi}(\sin\beta)^3\,d\beta$$

$$= \frac{1}{2\pi}(\pi+0+0) = 1/2$$

The method of averaging

Method of averaging

Add languages

Article Talk Read Edit View history Tools

From Wikipedia, the free encyclopedia

In mathematics, more specifically in dynamical systems, the **method of averaging** (also called averaging theory) exploits systems containing time-scales separation: a *fast oscillation* **versus** a *slow drift*. It suggests that we perform an averaging over a given amount of time in order to iron out the fast oscillations and observe the qualitative behavior from the resulting dynamics. The approximated solution holds under finite time inversely proportional to the parameter denoting the slow time scale. It turns out to be a customary problem where there exists the trade off between how good is the approximated solution balanced by how much time it holds to be close to the original solution.

More precisely, the system has the following form

$$\dot{x} = \varepsilon f(x, t, \varepsilon), \quad 0 \leq \varepsilon \ll 1$$

of a phase space variable x.The *fast oscillation* is given by f **versus** a *slow drift* of $\dot{x}$. The averaging method yields an autonomous dynamical system

$$\dot{y} = \varepsilon \frac{1}{T} \int_0^T f(y, s, 0)\, ds =: \varepsilon \bar{f}(y)$$

which approximates the solution curves of $\dot{x}$ inside a connected and compact region of the phase space and over time of $1/\varepsilon$.

Schematically

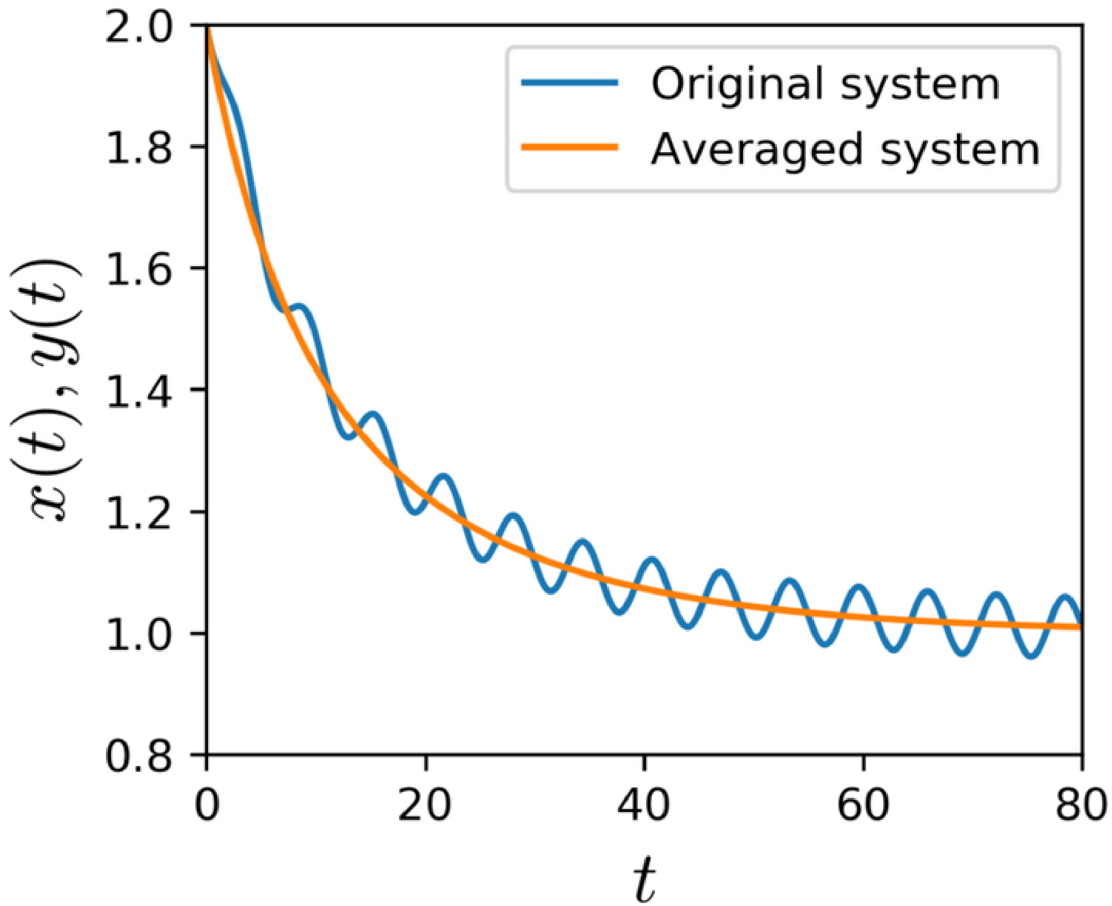

Figure 1: Solution to perturbed logistic growth equation $\dot{x} = \varepsilon(x(1-x) + \sin t)\ x \in \mathbb{R},\ \varepsilon = 0.05$ (blue solid line) and the averaged equation $\dot{y} = \varepsilon y(1-y),\ y \in \mathbb{R}$ (orange solid line).

We can predict the <u>average</u> drift in longitude

$$\frac{d\Omega}{d\beta}_{AVG} = \frac{-3J_2{R_\oplus}^2}{2(a(1-e^2))^2}\cos i$$

$$\Downarrow$$

$$\dot{\Omega}_{AVG} \cong \frac{d\Omega}{d\beta}_{AVG}\left(\frac{h}{r^2}\right)_{AVG} = \frac{d\Omega}{d\beta}_{AVG}\frac{2\pi}{T} = \frac{d\Omega}{d\beta}_{AVG}\sqrt{\frac{\mu}{a^3}}$$

Mean angular rate

$$\Downarrow$$

$$\boxed{\dot{\Omega}_{AVG} \cong -\left[\frac{3}{2}\frac{J_2{R_\oplus}^2\sqrt{\mu}}{(1-e^2)^2a^{7/2}}\right]\cos i}$$

$0 \leq i \leq 90°,\ \dot{\Omega} < 0$

The node line drifts westward

$i = 90°,\ \dot{\Omega} = 0$

The node line is stationary

Let's check for polar orbits!

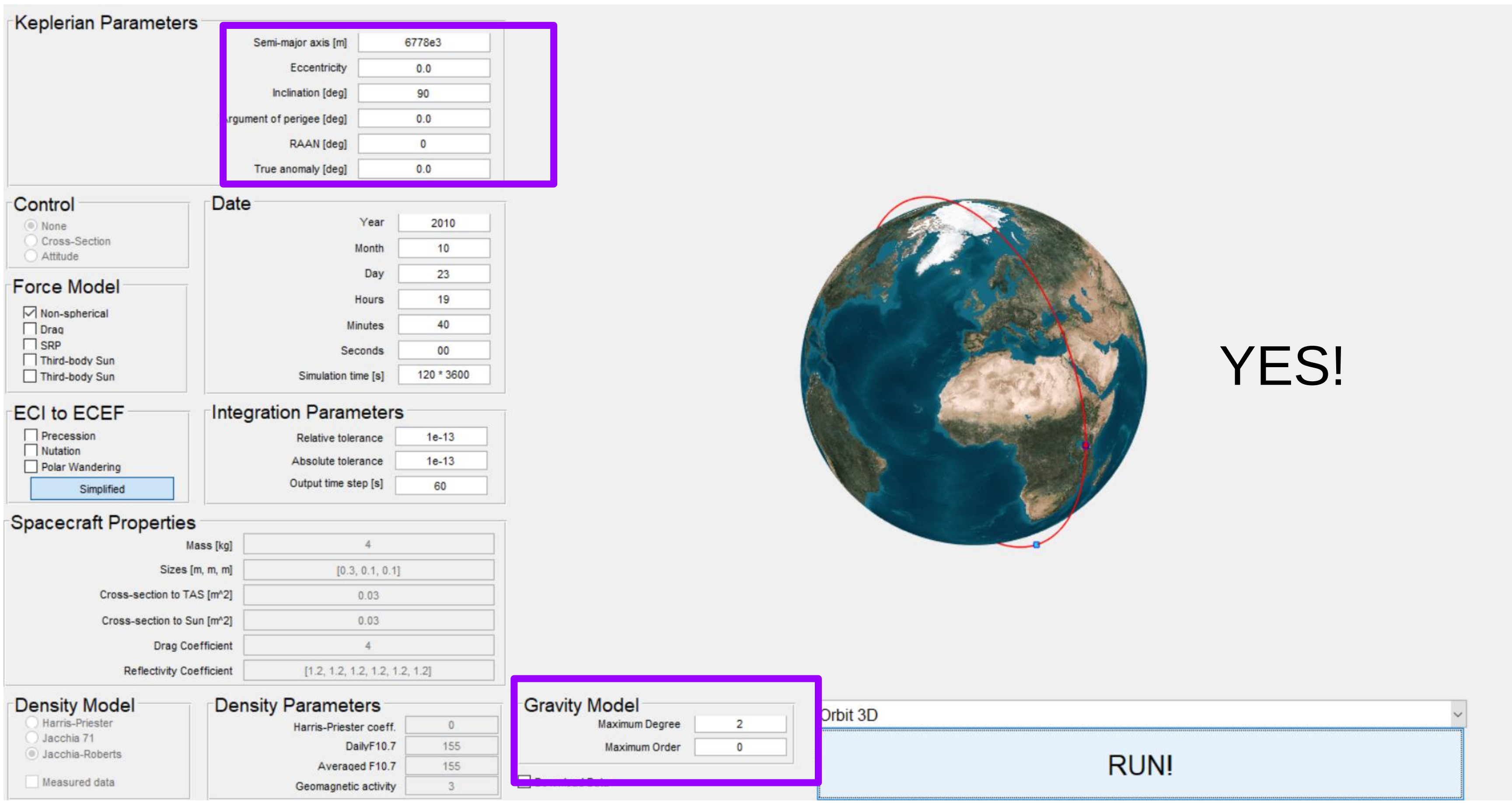

Analytical prediction: the ISS case

```
>> i=51/180*pi;a=(6378+400)*1e3;muu=3.98600e14;J2=0.00108;R=6378e3;
>> omegadot=[-1.5*sqrt(muu)*J2*R^2/(a^3.5)*cos(i)]/pi*180*86400

omegadot =

   -5.0560
```

Analytical prediction: the drift in longitude for the ISS is 5 degrees per day

Analytical prediction: the ISS case

Physical interpretation of the J2 perturbation

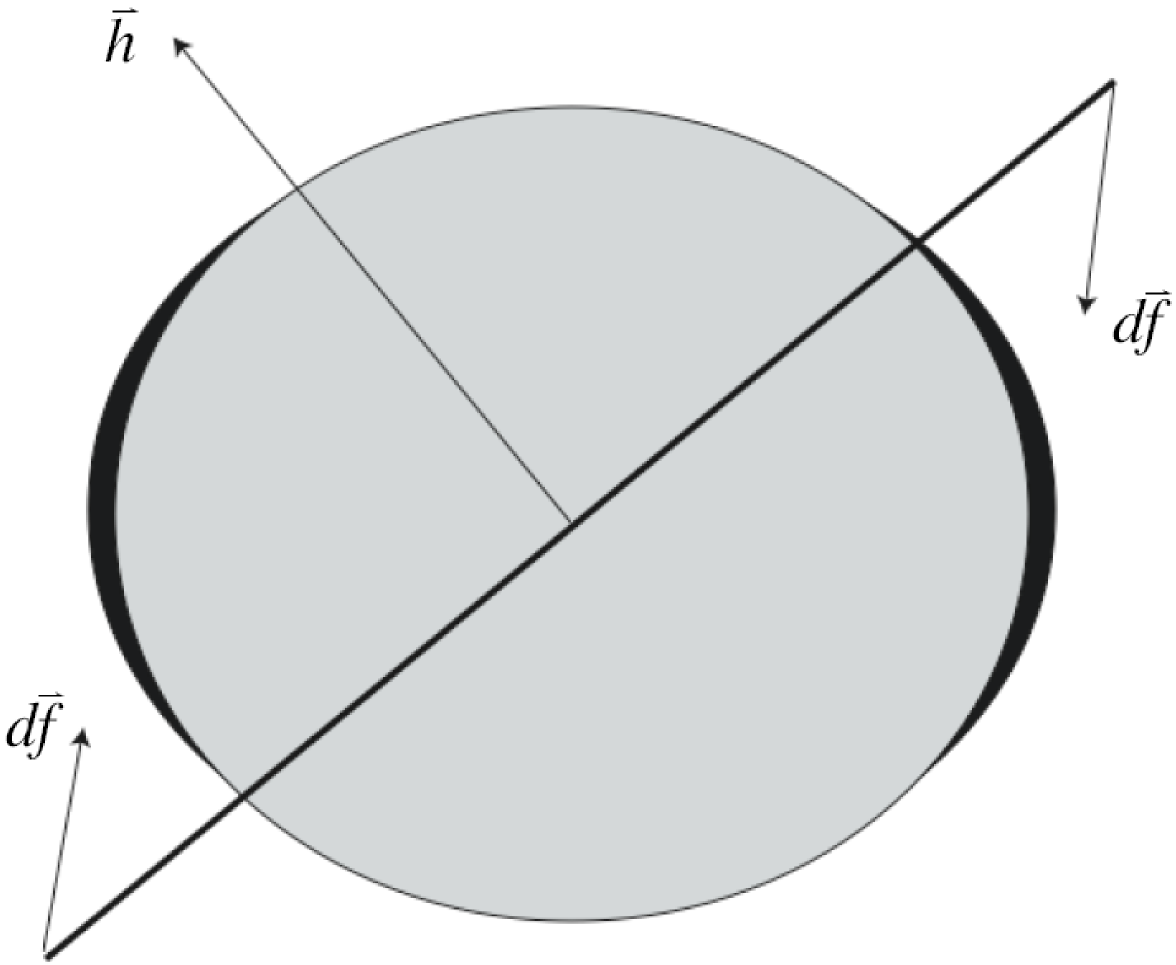

$$\ddot{\vec{r}} = -\frac{\mu\vec{r}}{r^3} + d\vec{f}$$

$$\vec{r}\times\ddot{\vec{r}} = -\vec{r}\times\frac{\mu\vec{r}}{r^3} + \vec{r}\times d\vec{f}$$

$$\frac{d}{dt}\left(\vec{r}\times\dot{\vec{r}}\right) = \dot{\vec{h}} = \vec{r}\times d\vec{f}$$

Physical interpretation of the perturbation

The oblateness means that the force of gravity is no longer within the orbital plane: **non-planar motion will result**.

The equatorial bulge exerts a force that pulls the satellite back to the equatorial plane and thus tries to align the orbital plane with the equator.

Due to its angular momentum, the orbit behaves like a spinning top and reacts with a precessional motion of the orbital plane (the orbital plane of the satellite to rotate in inertial space).

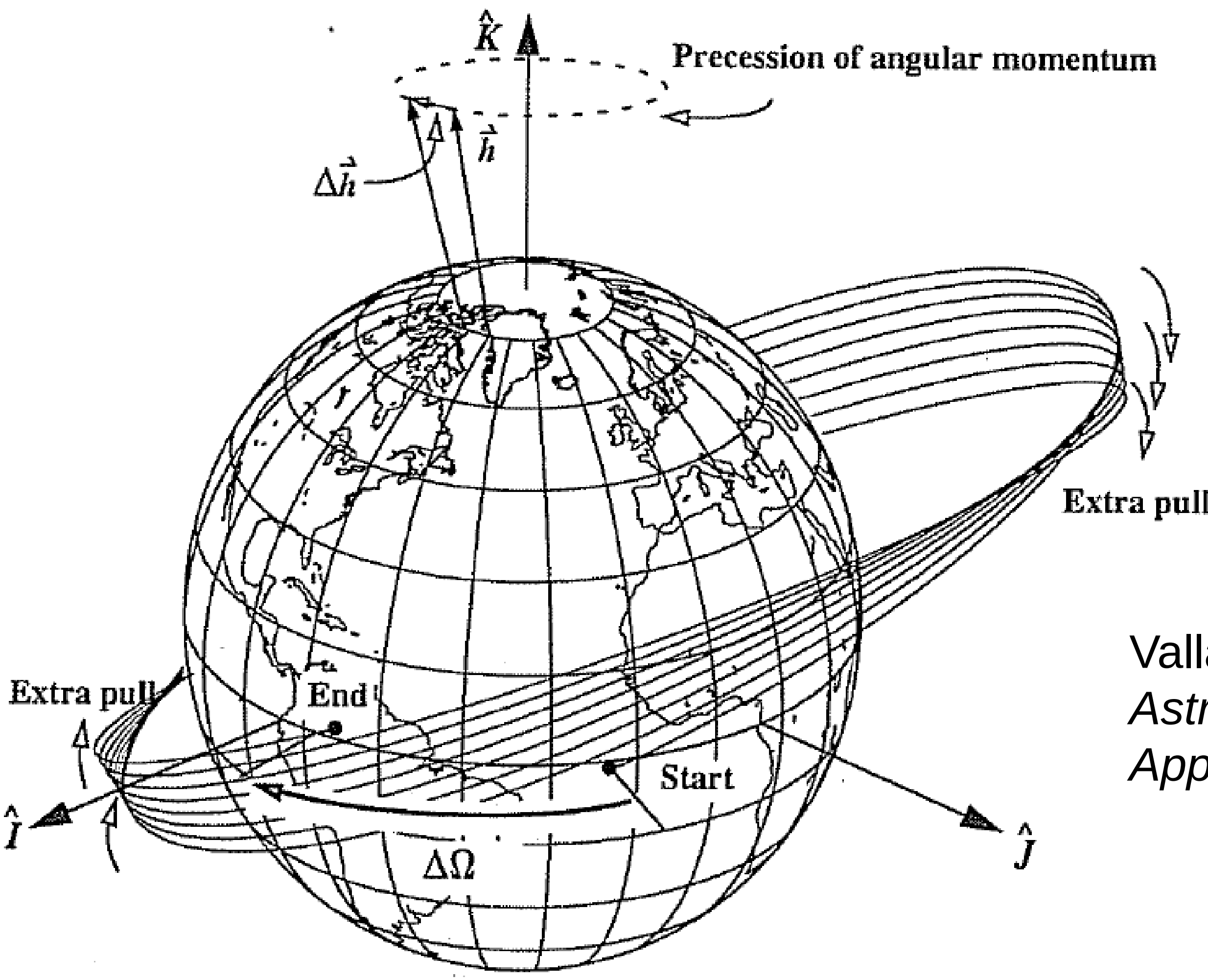

Vallado, *Fundamental of Astrodynamics and Applications*, Kluwer, 2001.

How Nodal Regression Works. The effect of a J_2 perturbation that is 20 times the real value of J_2 shows the precession of the longitude of ascending node. The perturbation manifests itself through a change in the angular-momentum vector, and the node regresses much like a precessing top. For this example, the correct interpretation is to say that the satellite's line of nodes experiences a rotation of 50/8° per revolution, or 50° per unit of time. The figure is also distorted because there is some apsidal rotation with an inclination not at the critical inclination (63.4°).

Can we exploit the drift in longitude ?

The orbital plane makes a constant angle with the radial from the sun:

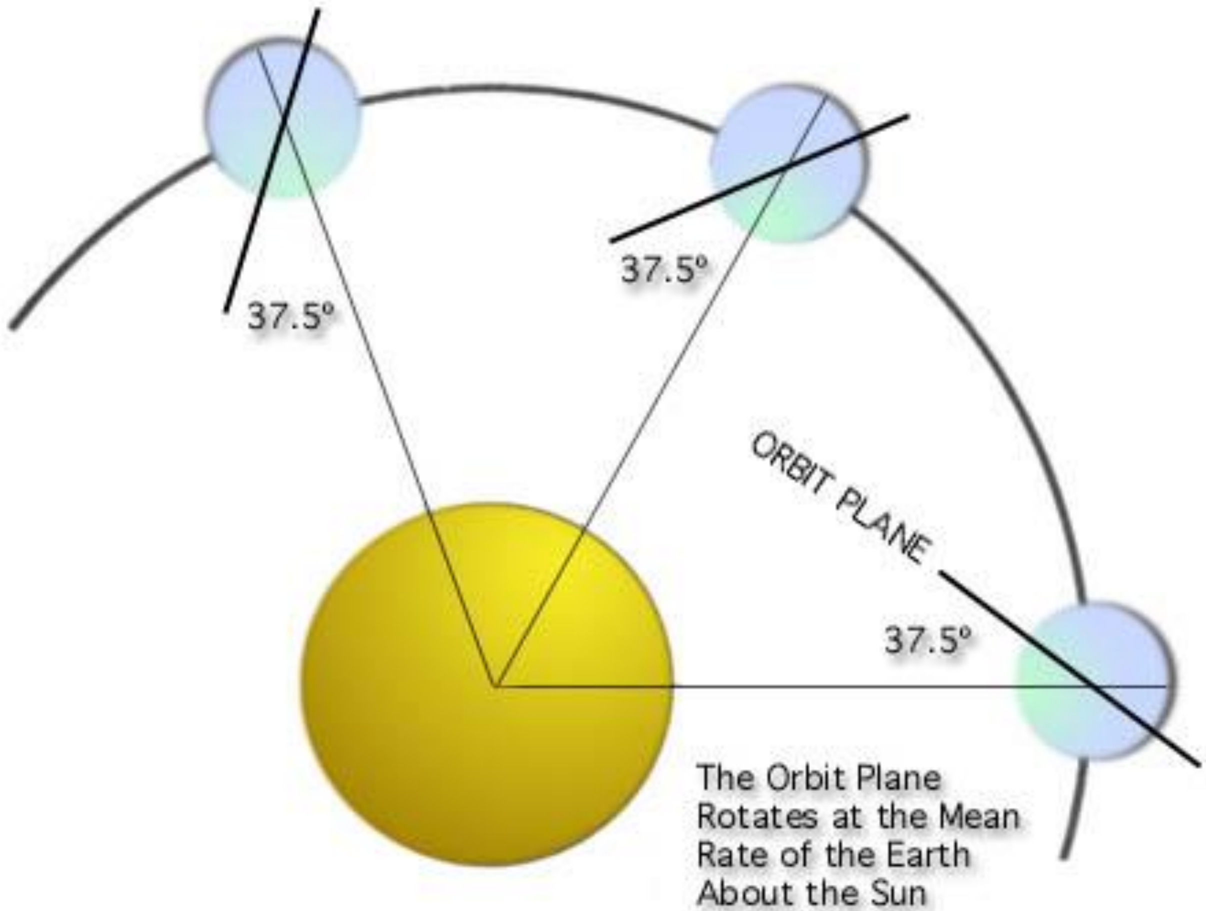

Yes ! Sun-synchronous orbits

The orbital plane must rotate in inertial space with the angular velocity of the Earth in its orbit around the Sun:

360º per 365.26 days or 0.9856º per day

The satellite sees any given swath of the planet under nearly the same condition of daylight or darkness day after day.

Example of SPOT-5 satellite


```
>> i=98.7/180*pi;a=(6378+820)*1e3;muu=3.98600e14;J2=0.00108;R=6378e3;
>> omegadot=[-1.5*sqrt(muu)*J2*R^2/(a^3.5)*cos(i)]/pi*180*86400

omegadot =

    0.9846
```

Effect of perturbations on orbital elements

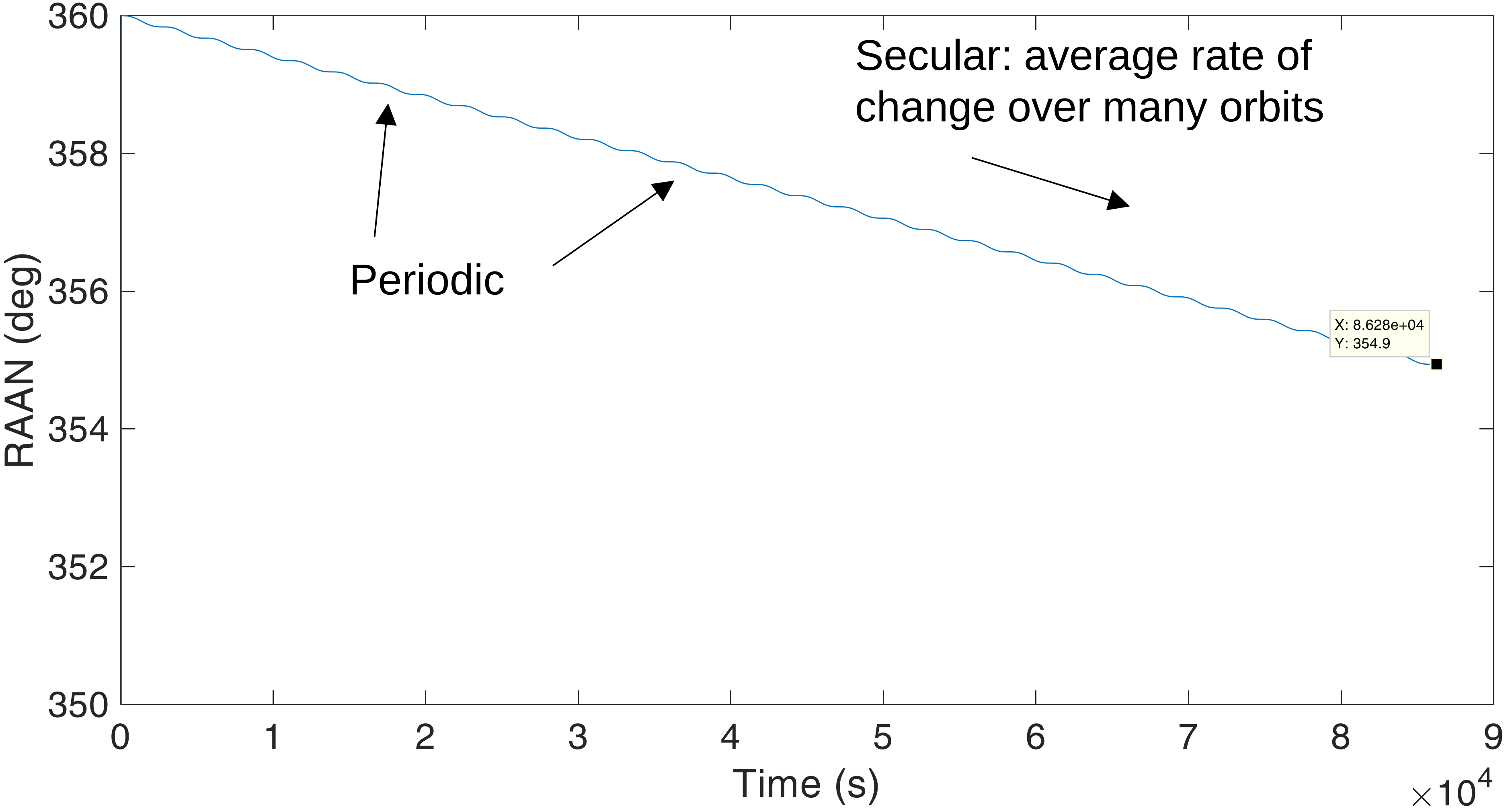

Secular effects: apse line

$$\dot{\omega}_{avg} = \frac{1}{T}\int_0^T \dot{\omega}\, dt = \left[\frac{3}{4}\frac{\sqrt{\mu}J_2R^2}{(1-e^2)^2 a^{7/2}}\right]\left(4-5\sin^2 i\right)$$

$$0^\circ \le i \le 63.4^\circ \text{ or } 116.6^\circ \le i \le 180^\circ,\ \dot{\omega} > 0$$

$\Rightarrow$ The perigee advances in the direction of the motion of the satellite. And conversely.

$$i = 63.4^\circ \text{ or } i = 116.6^\circ,\ \dot{\omega} = 0$$

$\Rightarrow$ The apse line does not move.

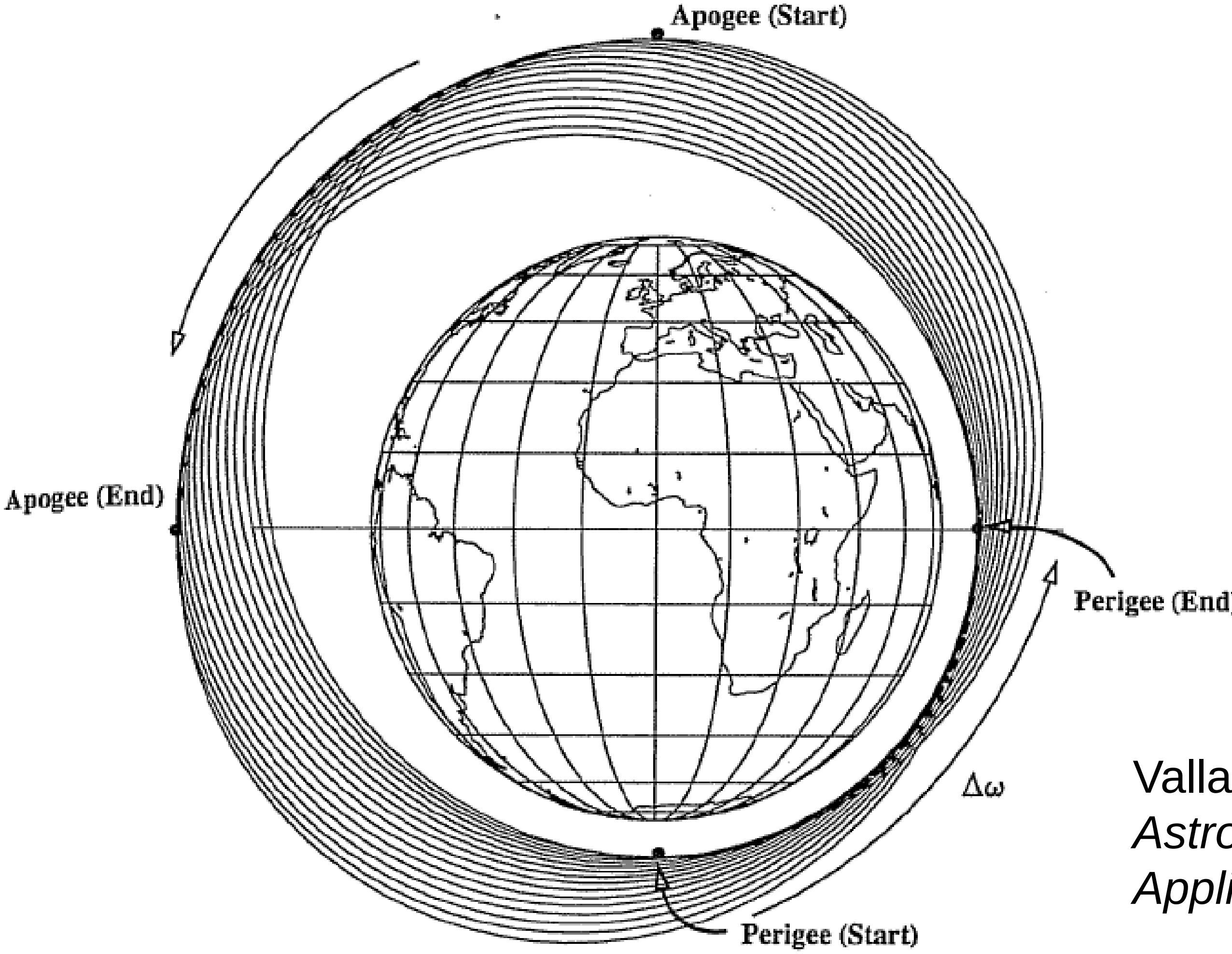

Vallado, *Fundamental of Astrodynamics and Applications*, Kluwer, 2001.

Figure 9-5. **How Apsidal Rotation Works.** We can see the effect of apsidal rotation after the J_2 perturbation effect increases by a factor of 40 for a polar orbit (to eliminate the nodal regression). Notice how perigee (and apogee) locations change dramatically in a few revolutions.

Can we exploit the drift of the perigee ?

A geostationary satellite cannot view effectively the far northern latitudes into which Russian territory extends (+ costly plane change maneuver for the launch vehicle !)

Molniya telecommunications satellites are launched from Plesetsk (62.8ºN) into 63º inclination orbits having a period of 12 hours.

$$T_{ellip} = 2\pi\sqrt{\frac{a^3}{\mu}} \rightarrow \text{ the apse line is 53000 km long.}$$

US-KS satellites (Russia)

Payload: early warning detection of rocket launches from the US.

40000 x 600 kms, Molniya (i=63.4°, T=12h)

Demanding environment: radiation

Satellite: shut down electronic equipment


-150
-120
-90
-60
-30
0
30
60
90
120
150

Analytic propagators in STK: 2-body, J2

2-body: constant orbital elements.

J2: accounts for secular variations in the orbit elements due to Earth oblateness; periodic variations are neglected.

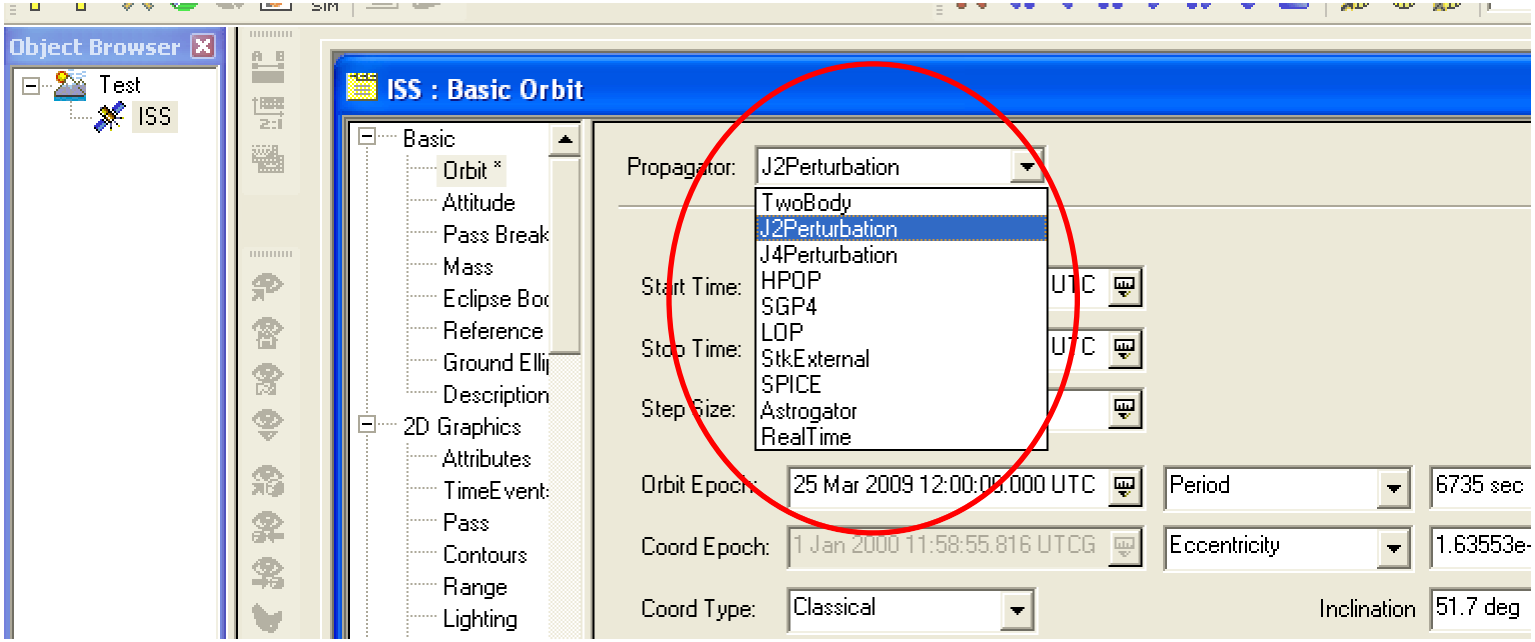

J2 propagator: underlying equations

$$\bar{n} = n\left[1 + \frac{3}{2} J_2 \frac{R_e^2}{p^2}\sqrt{1-e^2}\left(1 - \frac{3}{2}\sin^2 i\right)\right]$$

$$\omega = \omega_0 + \left(\frac{3}{2} J_2 \frac{R_e^2}{p^2}\left[2 - \frac{5}{2}\sin^2 i\right]\right)\bar{n}(t - t_0)$$

$$\Omega = \Omega_0 - \left(\frac{3}{2} J_2 \frac{R_e^2}{p^2}\cos i\right)\bar{n}(t - t_0)$$

$$M = M_0 + \bar{n}(t - t_0)$$

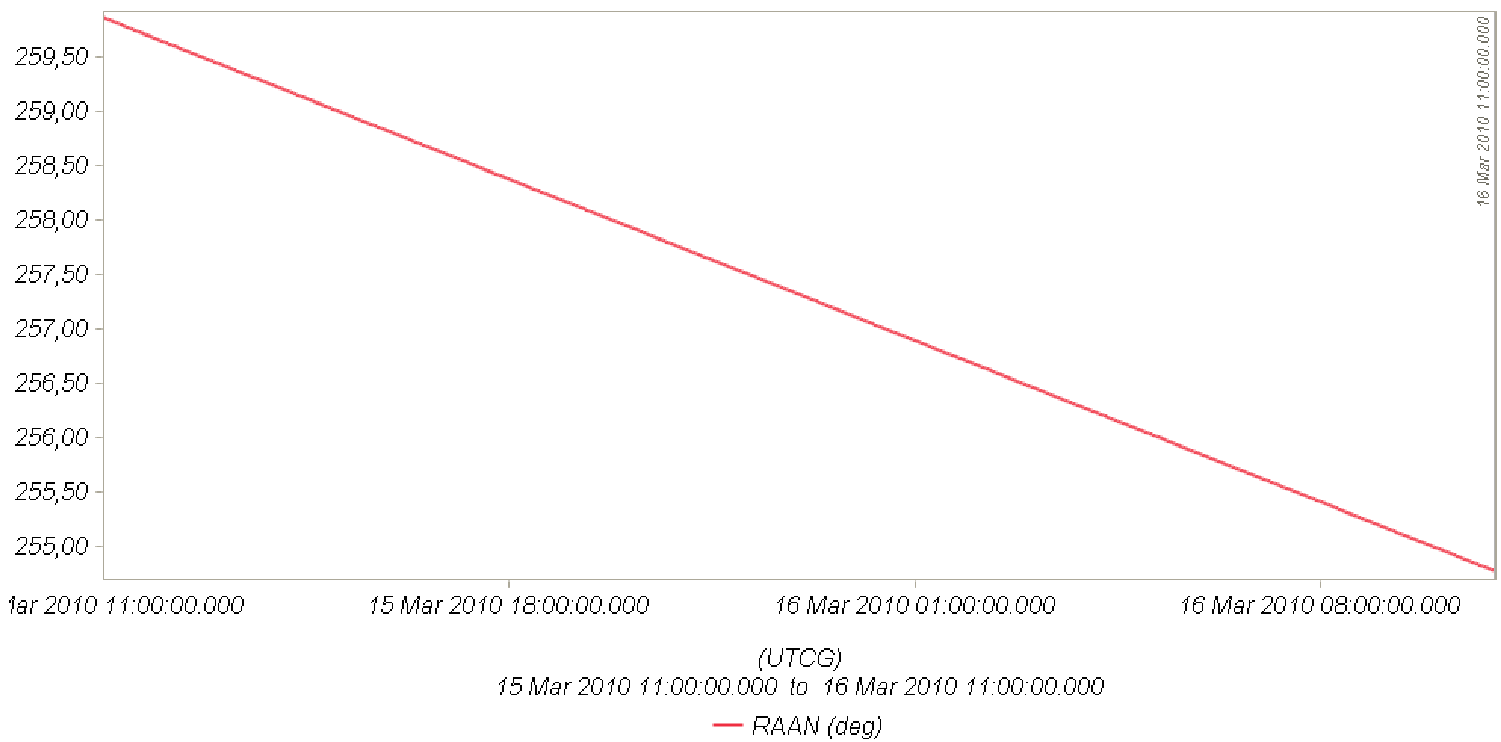

HPOP and J2 propagators applied to ISS

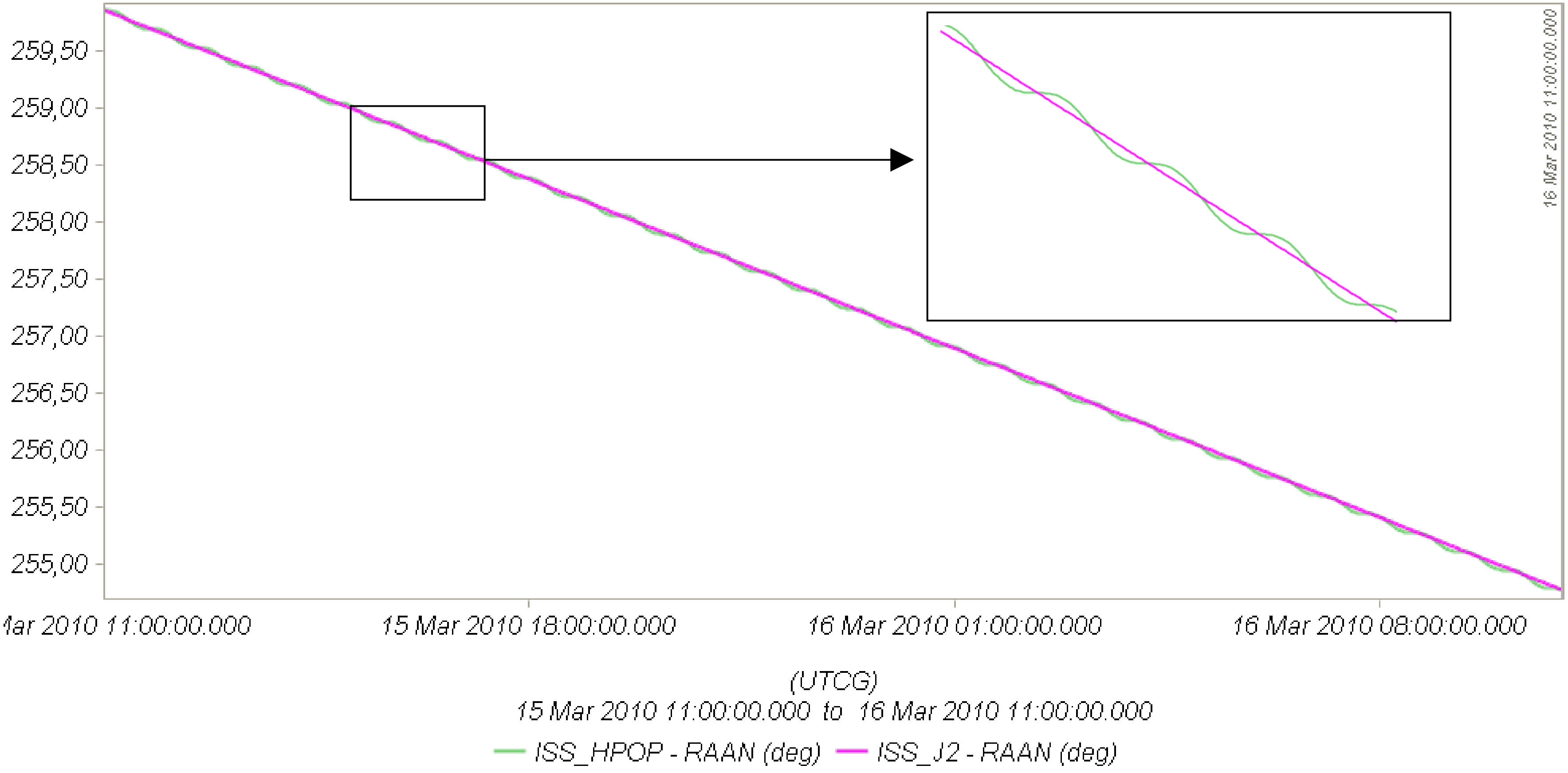

Effects of atmospheric drag: semi-major axis

$$\dot{a} = \frac{\mu}{2\varepsilon^2}\dot{\varepsilon} = \underbrace{\frac{2a^2}{\mu}}_{>0}\dot{\varepsilon}$$

Because drag causes the dissipation of mechanical energy from the system, the semimajor axis contracts.

Drag paradox: the effect of atmospheric drag is to increase the satellite speed and kinetic energy !

Effects of atmospheric drag : semi-major axis

$$N = R = 0, \quad T = -\frac{1}{2} C_D \frac{A}{m} \rho v_r^2 = -\frac{1}{2} C_D \frac{A}{m} \rho \frac{\mu}{a}$$

$$\dot{a} = 2\sqrt{\frac{a^3}{\mu\left(1-e^2\right)}}\left[\mathrm{R}\sin\theta + T\left(1+e\cos\theta\right)\right]$$

Circular orbit

$$\dot{a} = -\sqrt{a\mu}\,\rho C_D \frac{A}{m} < 0$$

ρ is assumed constant

$$\boxed{\sqrt{a_f} - \sqrt{a_i} = \frac{-\sqrt{\mu}\,\rho C_D A}{2m}\left(t_f - t_i\right)}$$

Effects of atmospheric drag : orbital plane

$$\dot{\Omega} = \sqrt{\frac{a(1-e^2)}{\mu}} \frac{N \sin\theta_2}{\sin i \left(1 + e\cos\theta\right)}$$

$$\dot{i} = \sqrt{\frac{a(1-e^2)}{\mu}} \frac{N \cos\theta_2}{\left(1 + e\cos\theta\right)}$$

$$\Downarrow$$

The orientation of the orbit plane is not changed by drag.

Effects of atmospheric drag: apogee, perigee

Apogee height changes drastically, perigee height remains relatively constant.

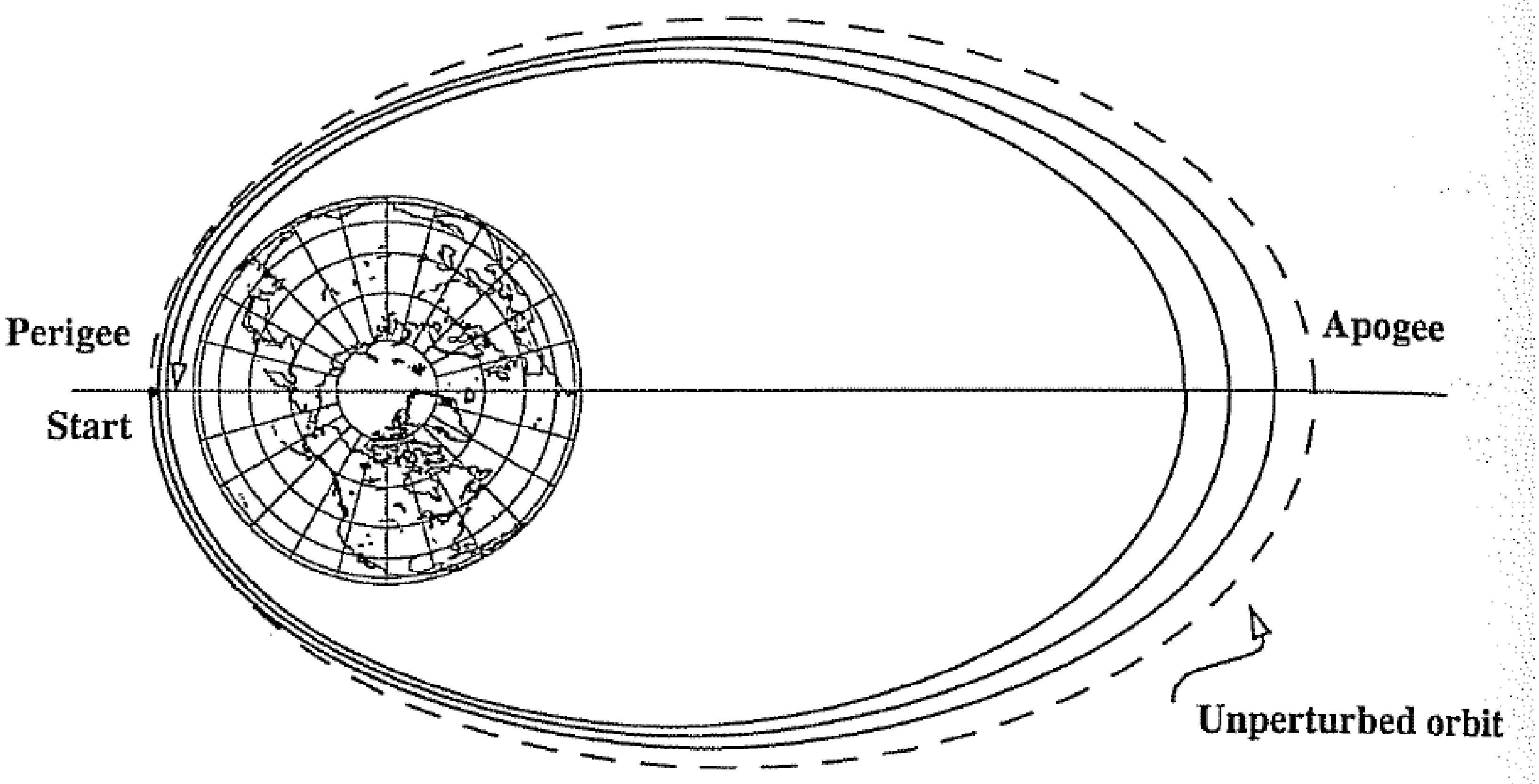

Vallado, *Fundamental of Astrodynamics and Applications*, Kluwer, 2001.

Effects of atmospheric drag : eccentricity

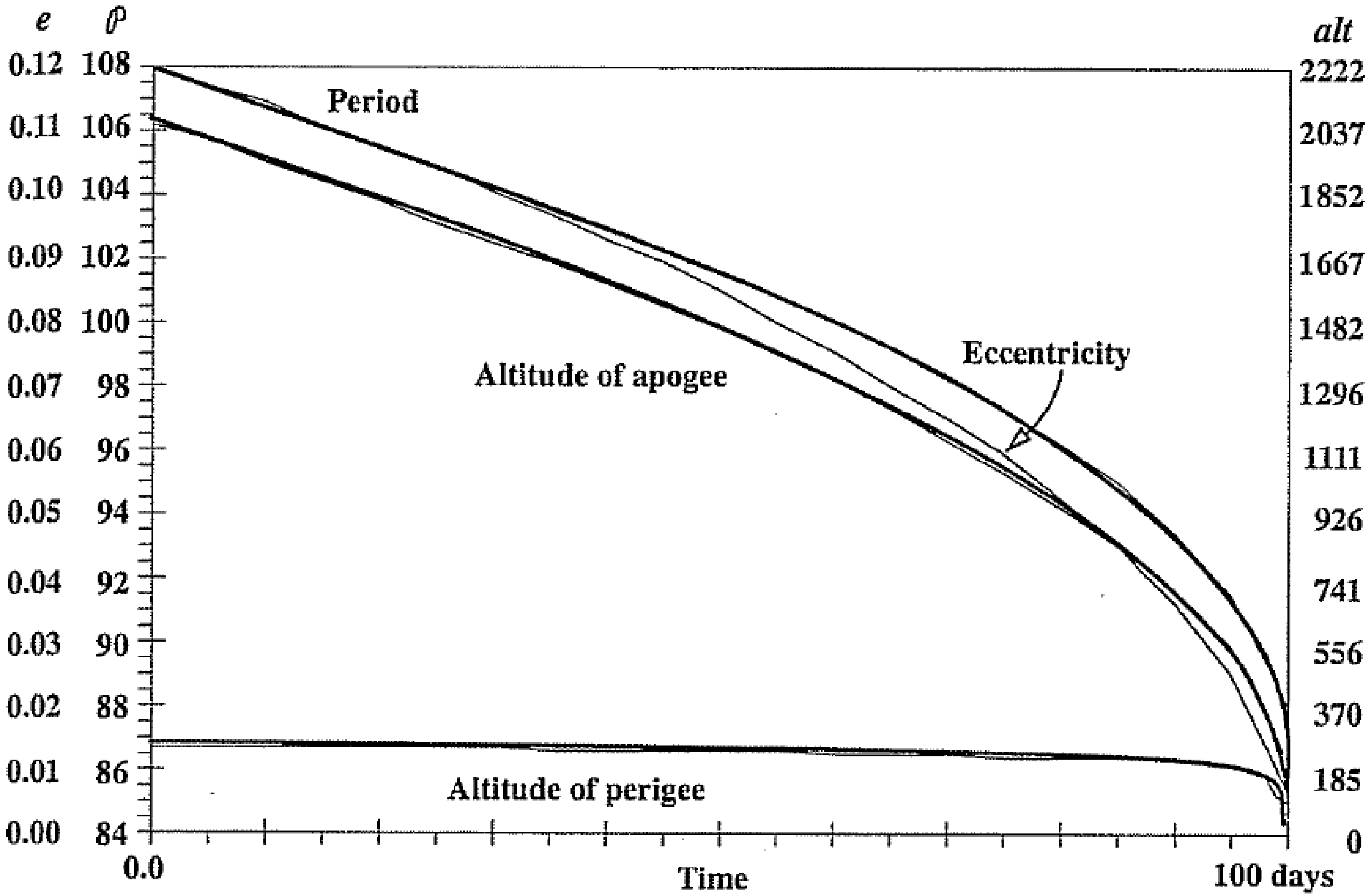

Vallado, *Fundamental of Astrodynamics and Applications*, Kluwer, 2001.

Early reentry of Skylab (1979)

Increased solar activity, which increased drag on Skylab, led to an early reentry.

Earth reentry footprint could not be accurately predicted (due to tumbling and other parameters).

Debris was found around Esperance (31–34°S, 122–126°E). The Shire of Esperance fined the United States $400 for littering, a fine which, to this day, remains unpaid.

Effects of third-body perturbations

The only secular perturbations are in the node and in the perigee.

For near-Earth orbits, the dominance of the oblateness dictates that the orbital plane regresses about the polar axis. For higher orbits, the regression will be about some mean pole lying between the Earth's pole and the ecliptic pole.

Many geosynchronous satellites launched 30 years ago now have inclinations of up to $\pm 15^{o}$ $\Rightarrow$ collision avoidance as the satellites drift back through the GEO belt.

Effects of third-body perturbations

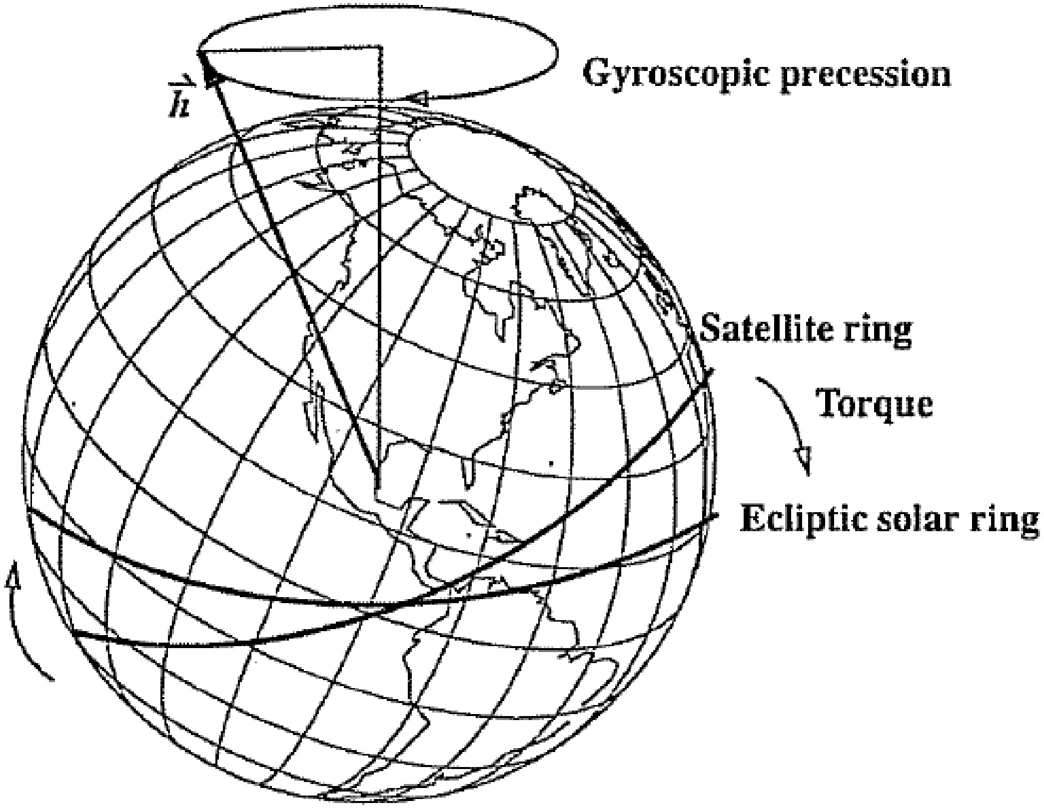

The Sun's attraction tends to turn the satellite ring into the ecliptic. The orbit precesses about the pole of the ecliptic.

Third-Body Interactions. Imagine that the entire mass of a third body (the Sun, for instance) occupies a band about the planet. The resulting torque causes the satellite's orbit to precess like a gyroscope.

Vallado, *Fundamental of Astrodynamics and Applications*, Kluwer, 2001.

STK: analytic propagator (SGP4)

The J2 propagator does not include drag.

SGP4, which stands for Simplified General Perturbations Satellite Orbit Model 4, is a NASA/NORAD algorithm.

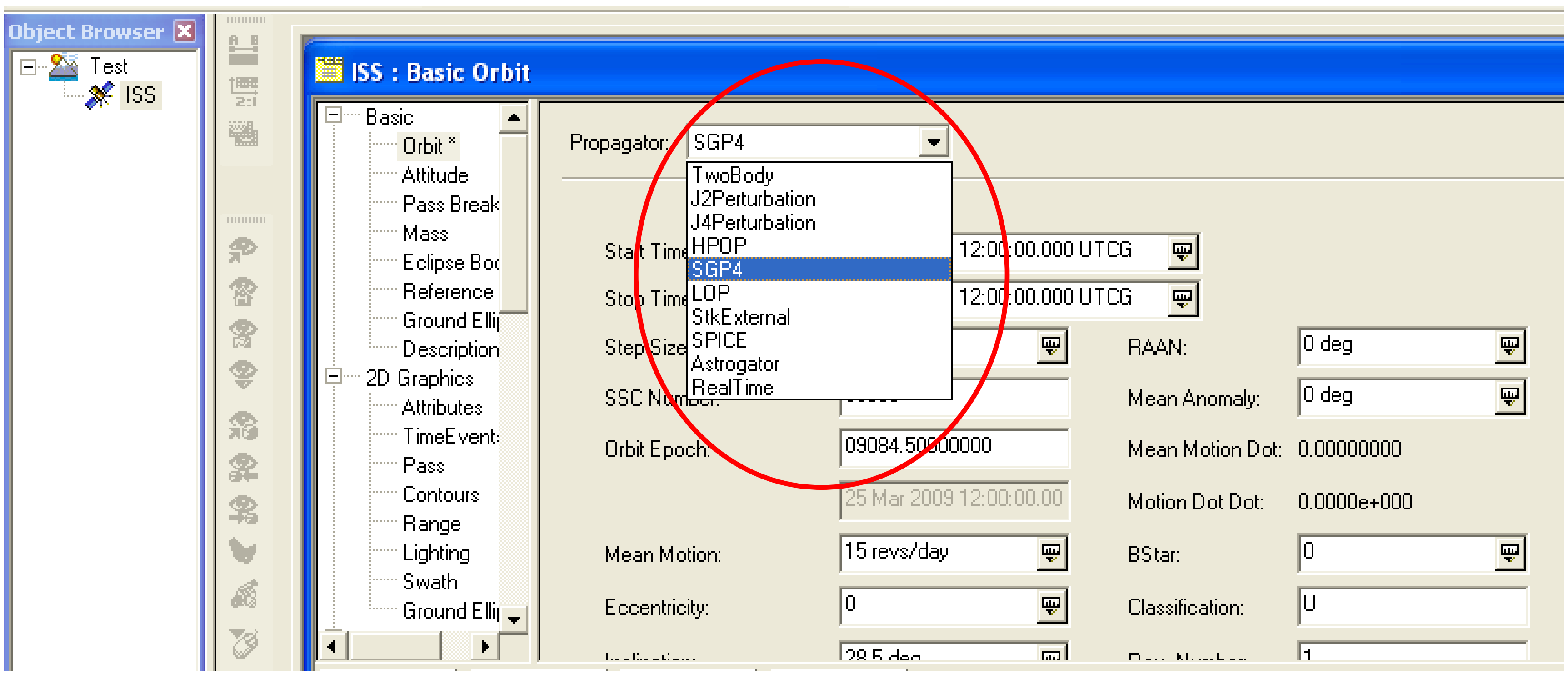

STK: analytic propagator (SGP4)

Several assumptions; propagation valid for short durations (3-10 days).

TLE data should be used as the input.

It considers secular and periodic variations due to Earth oblateness, solar and lunar gravitational effects, and orbital decay using a drag model.

SGP4 applied to ISS: RAAN

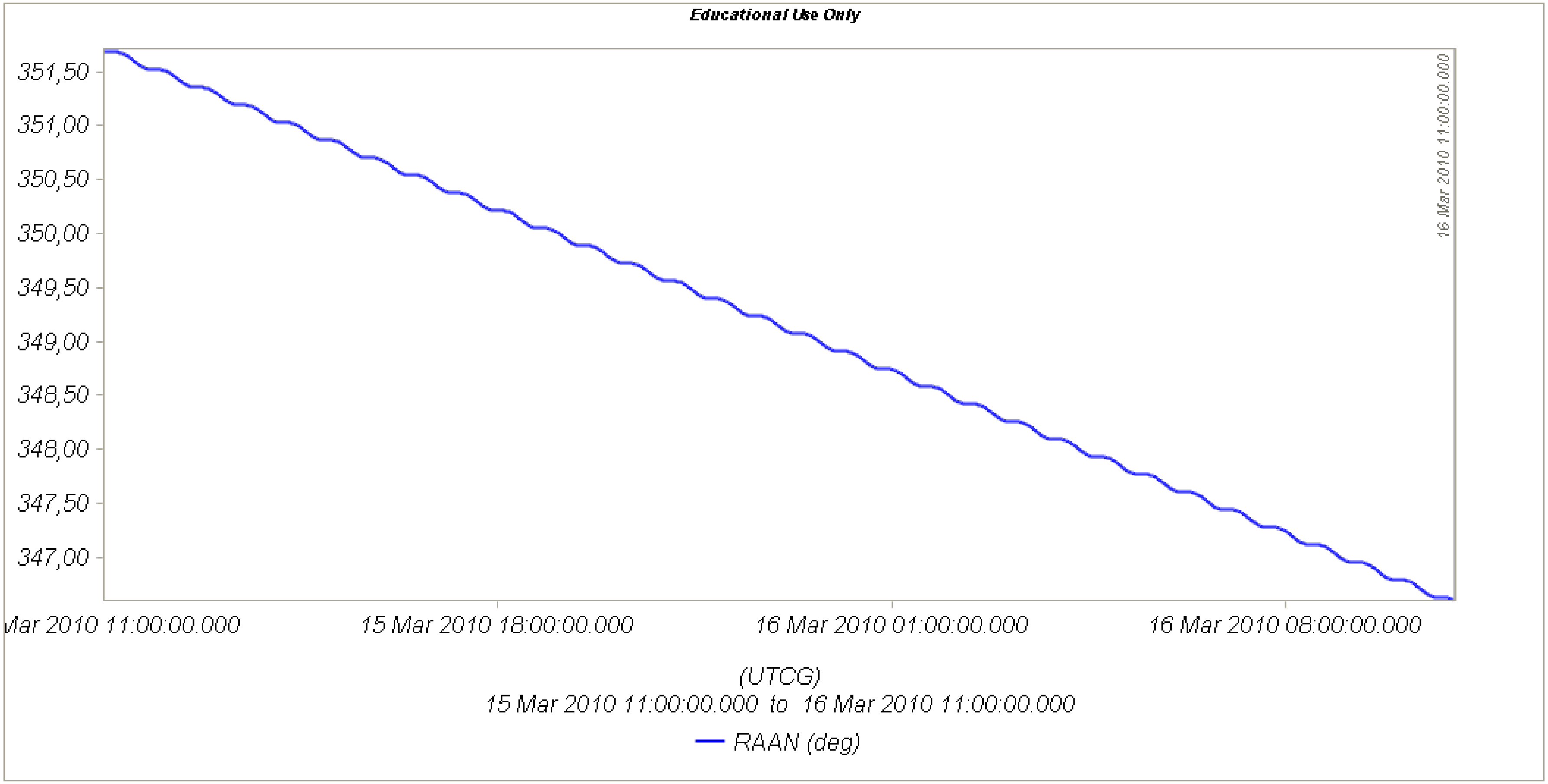

Further reading

SPACETRACK REPORT NO. 3

Models for Propagation of NORAD Element Sets

Felix R. Hoots
Ronald L. Roehrich

Secular effects: orders of magnitude

Orbit Class	Central Body		Drag	
Secular Effects	Ω °/day	ω °/day	a m/day	e /day
LEO	–5.7	6.5	5000	
Shuttle	–5	5		
Mir	–5.0	3.8		
Landsat	1	–3.1	100	
DMSP	1	–2.9		
TOPEX	–2.1	–0.5		
LAGEOS I	0.3	–0.2		
ICO	–0.1	0.1		
GPS	~	~		
Molniya	–0.2		100	

Vallado, *Fundamental of Astrodynamics and Applications*, Kluwer, 2001.

Periodic effects: orders of magnitude

Orbit Class	Central Body				Drag	Third Body	Solar Radiation
Periodic Effects	SP	m-daily	lin com	Res			
	m	m	m	m	m	m	m
LEO							
Shuttle	7000	470	50	Deep	33	0.5	~
Mir	6000	380	46		3	0.3	~
Landsat	9100	610	36		~	~	~
DMSP	9000	590	134		~	~	~
TOPEX	7200	445	334		~	1	~
LAGEOS I	4800	115	18			0.1	~
ICO	2000	40	23			10	10
GPS	1700	17	18	Deep		100	12
Molniya	32,000	105	900	Deep	50	250	10
GEO	1600	~	16	Deep		716	50

Vallado, *Fundamental of Astrodynamics and Applications*, Kluwer, 2001.

Orbital propagation

$$\dot{\Omega} = \sqrt{\frac{a(1-e^2)}{\mu}}\,\frac{N \sin\theta_2}{\sin i\left(1+e\cos\theta\right)}$$

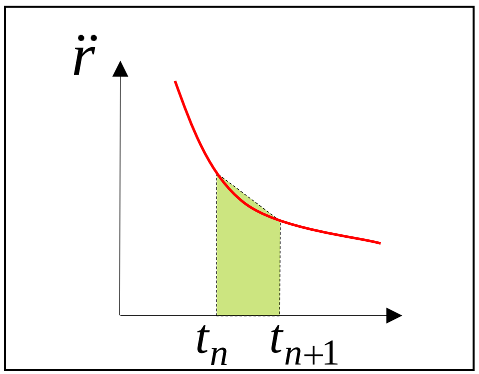

Numerical methods

STK propagators

2-body: analytic propagator (constant orbital elements).

J2: analytic propagator (secular variations in the orbit elements due to Earth oblateness.

HPOP: **numerical integration** of the equations of motion (periodic and secular effects included).

✓ Accurate

✓ Versatile

✗ Errors accumulation for long intervals

✗ Computationally intensive

Real-life example: German aerospace agency

ANALYSIS OF ORBIT PROPAGATION AND RELATIVE POSITION ACCURACY OF SMALL SATELLITES FOR SAR INTERFEROMETRY

Sergio De Florio, Dr. Thomas Neff, Tino Zehetbauer
DLR, Microwave and Radar Institute, Oberpfaffenhofen
Münchner Straße 20, 82234 Weßling, Germany
Phone: +498153282357, Fax: +498153281452, Sergio.DeFlorio@dlr.de

Earth gravity field model	70x70 gravity coefficients of the 200x200 GRACE-GGM02C gravity model
Third body gravitational perturbation	Sun and Moon using highly accurate planetary ephemeris DE200 generated by JPL
Atmospheric density model	Jacchia-Roberts implemented with a $F_{10.7}$ (10.7 cm solar flux index) prediction file
Numerical integration	Runge Kutta 8(9) algorithm

Real-life example: German aerospace agency

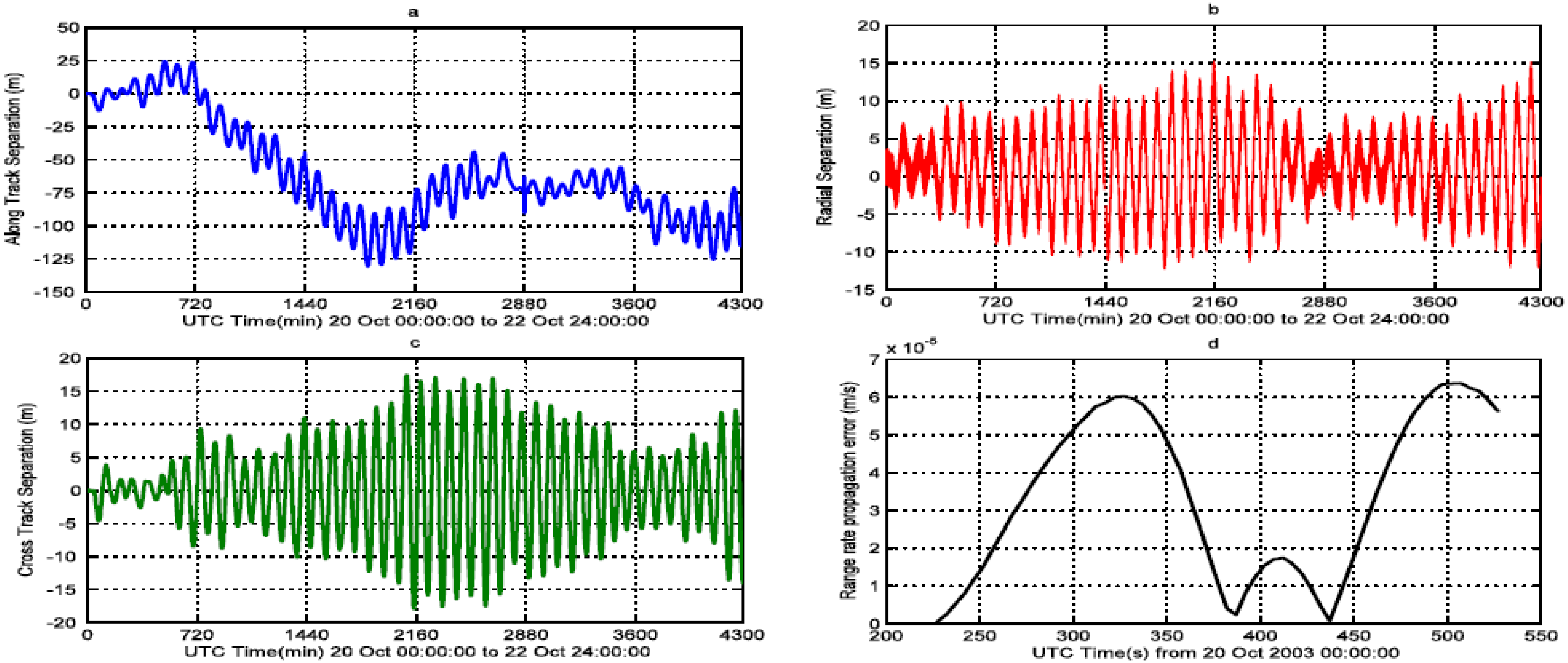

Figure 3. Propagation errors

propagation tool. The accuracy which can be reached with the presented method, after a propagation of 3 days, is about 10 – 15 m RMS in cross-track and radial direction and about 100 m RMS in along-track direction.

Further reading

IMPACT OF ORBIT PREDICTION ACCURACY ON LOW EARTH REMOTE SENSING FLIGHT DYNAMICS OPERATIONS

Christian Arbinger[(1)], Simone D'Amico[(1)]

[(1)]*German Space Operations Center (DLR/GSOC), D-82234 Wessling (Germany), E-mail: christian.arbinger@dlr.de*

This paper addresses the problem of orbit prediction and its impact on flight dynamics operations. In general, certain "knowledge" of the satellite's orbit is necessary to design and implement a ground-in-the-loop orbit control system. The operational constraints imposed by Low Earth Orbit (LEO) satellites and the stringent orbit control requirements driven by the use synthetic-aperture-radars (SAR) on board the satellites, give great importance to the orbit calculation chain.

Real-life example: Envisat

Envisat Orbit Prediction Error

The following table shows the RMS of the daily computed **along-track** errors over 1 orbit after 1, 3, and 6 days of Envisat orbit prediction.

Envisat (meters)

Month	after 1 day	after 3 days	after 6 days
December 2008	12	49	160
November 2008	12	54	194
October 2008	11	46	148
September 2008	11	38	128
August 2008	11	50	159
July 2008	12	47	144
June 2008	12	45	161
May 2008	14	47	127
May 2008	14	47	127
April 2008	12	51	173
March 2008	11	42	122

http://nng.esoc.esa.de/envisat/ENVpred.html

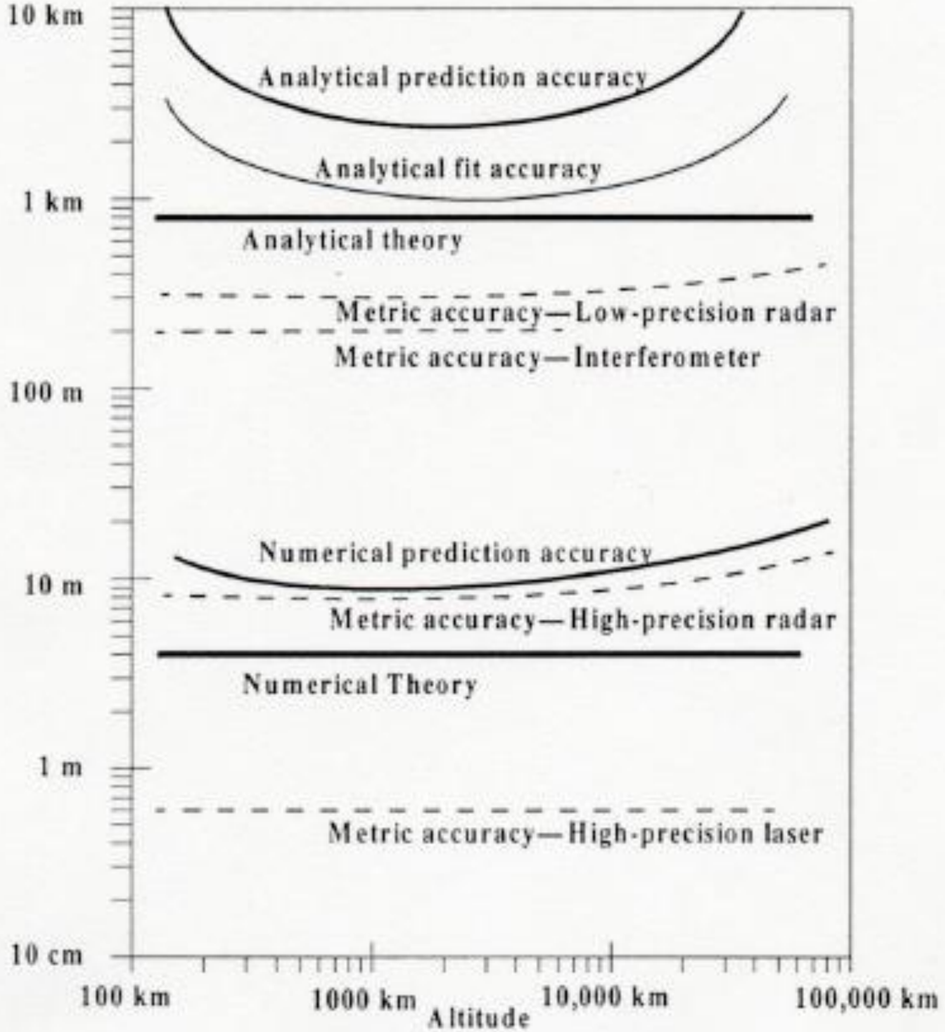

Errors in Determining a Satellite's Position. This figure (Knowles, 1995) shows general trends for typical accuracies of numerical and analytical theories (solid lines). Semianalytical theories range from nearly numerical to nearly analytical, depending on their force models. Observations (dashed lines) tend to degrade at higher altitudes. Notice how predictions and propagations degrade the theoretical accuracies, especially for analytical theories with significant drag and third-body effects.

Why do the predictions degrade for lower altitudes ?

Did you know ?

NASA began the first complex numerical integrations during the late 1960s and early 1970s.

1968

1969

What is numerical integration ?

Given

$$\left\{\begin{array}{l}\ddot{\mathbf{r}} = -\dfrac{\mu}{r^3}\mathbf{r} + \mathbf{a}_{perturbed} \\ \mathbf{r}(t_n), \dot{\mathbf{r}}(t_n) \\ \Delta t = t_{n+1} - t_n\end{array}\right.$$

Compute

$$\mathbf{r}(t_{n+1}), \dot{\mathbf{r}}(t_{n+1})$$

State-space formulation

$$\ddot{\mathbf{r}} = -\frac{\mu}{r^3}\mathbf{r} + \mathbf{a}_{perturbed}$$

$$\dot{\mathbf{u}} = f(\mathbf{u}, t) \qquad \mathbf{u} = \begin{pmatrix} \mathbf{r} \\ \dot{\mathbf{r}} \end{pmatrix}$$

6-dimensional
state vector

How to perform numerical integration ?

$$\mathbf{u}(t_n)$$

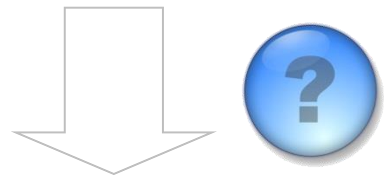

$$\mathbf{u}(t_{n+1})$$

$$f(t_n + h) = f(t_n) + hf\,'(t_n) + \frac{h^2}{2} f\,''(t_n) + \ldots + \frac{h^s}{s!} f^{(s)}(t_n) + R_s$$

Taylor series expansion

First-order Taylor approximation (Euler)

along the tangent

$$\mathbf{u}(t_n + \Delta t) = \mathbf{u}(t_n) + \boxed{\Delta t\, \dot{\mathbf{u}}(t_n)}$$

$$\mathbf{u}_{n+1} = \mathbf{u}_n + \Delta t\ f(\mathbf{u}_n, t_n)$$

Euler step

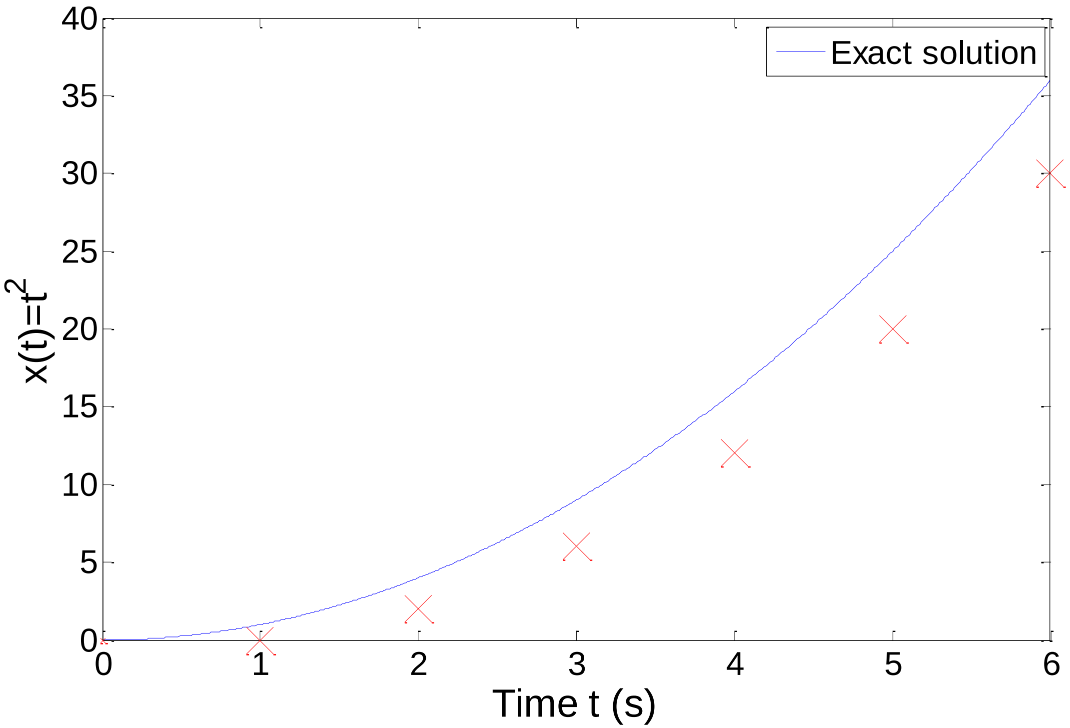

The stepsize has to be extremely small for accurate predictions, and it is necessary to develop more effective algorithms.

Numerical integration methods

$$\mathbf{u}_{n+1} = \sum_{j=1}^{m} \alpha_j \, \mathbf{u}_{n+1-j} - \Delta t \sum_{j=0}^{m} \beta_j \, \dot{\mathbf{u}}_{n+1-j}$$

State vector

$\beta_0 \neq 0$ — **Implicit**, the solution method becomes iterative in the nonlinear case

$\beta_0 = 0$ — **Explicit**, $\mathbf{u}_{n+1}$ can be deduced directly from the results at the previous time steps

$\alpha_j, \beta_j = 0$ for $j > 1$ — **Single-step**, the system at time t_{n+1} only depends on the previous state t_n

$\alpha_j, \beta_j \neq 0$ for $j > 1$ — **Multi-step**, the system at time t_{n+1} depends several previous states t_n,t_{n-1},etc.

Examples: implicit vs. explicit

$\Rightarrow$ Trapezoidal rule (implicit)

$$\mathbf{u}_{n+1} = \mathbf{u}_n + \Delta t \, \frac{\left(\dot{\mathbf{u}}_n + \dot{\mathbf{u}}_{n+1}\right)}{2}$$

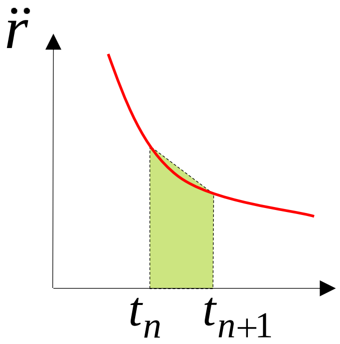

$\Rightarrow$ Euler backward (implicit)

$$\mathbf{u}_{n+1} = \mathbf{u}_n + \Delta t \, \dot{\mathbf{u}}_{n+1}$$

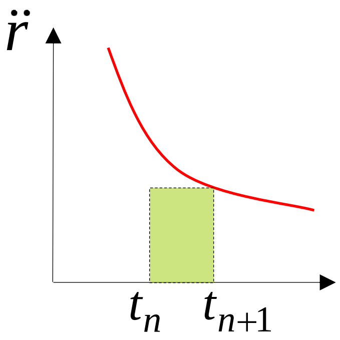

$\Rightarrow$ Euler forward (explicit)

$$\mathbf{u}_{n+1} = \mathbf{u}_n + \Delta t \, \dot{\mathbf{u}}_n$$

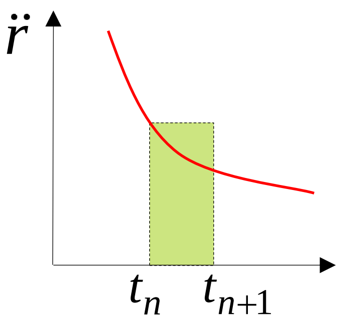

Why different methods ?

A variety of methods has been applied in astrodynamics. Each of these methods has its own advantages and drawbacks:

Accuracy:	what is the order of the integration scheme ?
Efficiency:	how many function calls ?
Versatility:	can it be applied to a wide range of problems ?
Complexity:	is it easy to implement and use ?
Step size:	automatic step size control ?

Runge-Kutta family: single-step

Perhaps the most well-known numerical integrator.

Difference with traditional Taylor series integrators: the RK family only requires the first derivative, but several evaluations are needed to move forward one step in time.

Different variants: explicit, embedded, etc.

Runge-Kutta family: single-step

$$\dot{\mathbf{u}}(t) = f(\mathbf{u}, t) \quad \text{with} \quad \mathbf{u}(t_0) = \mathbf{u}_0$$

$$\mathbf{u}_{n+1} = \mathbf{u}_n + \Delta t \sum_{i=1}^{s} b_i \mathbf{k}_i$$

Slopes at various points within the integration step

$$\mathbf{k}_1 = f\left(\mathbf{u}_n, t_n + c_1 \Delta t\right)$$

$$\mathbf{k}_i = f\left(\mathbf{u}_n + \Delta t \sum_{j=1}^{i-1} a_{ij} \mathbf{k}_j, t_n + c_i \Delta t\right), i = 2 \ldots s$$

Runge-Kutta family: single-step

The Runge-Kutta methods are fully described by the coefficients:

$$
\begin{array}{c|ccccc}
c_1 & & & & & \\
c_2 & a_{21} & & & & \\
\cdots & \cdots & \cdots & & & \\
c_s & a_{s1} & a_{s2} & \cdots & a_{s,s-1} & \\
\hline
 & b_1 & b_2 & \cdots & b_{s-1} & b_s
\end{array}
$$

Butcher Tableau

$$\sum_{i=1}^{s} b_i = 1$$

$$c_1 = 0$$

$$c_i = \sum_{j=1}^{i-1} a_{ij}$$

RK4 (explicit)

$$\mathbf{u}_{n+1} = \mathbf{u}_n + \Delta t \, \frac{\mathbf{k}_1 + 2\mathbf{k}_2 + 2\mathbf{k}_3 + \mathbf{k}_4}{6}$$

$$\mathbf{k}_1 = f\left(\mathbf{u}_n, t_n\right)$$

$$\mathbf{k}_2 = f\left(\mathbf{u}_n + \mathbf{k}_1 \frac{\Delta t}{2}, t_n + \frac{\Delta t}{2}\right)$$

$$\mathbf{k}_3 = f\left(\mathbf{u}_n + \mathbf{k}_2 \frac{\Delta t}{2}, t_n + \frac{\Delta t}{2}\right)$$

$$\mathbf{k}_4 = f\left(\mathbf{u}_n + \mathbf{k}_3 \Delta t, t_n + \Delta t\right)$$

$$\begin{array}{c|cccc}
0 & 0 & 0 & 0 & 0 \\
1/2 & 1/2 & 0 & 0 & 0 \\
1/2 & 0 & 1/2 & 0 & 0 \\
1 & 0 & 0 & 1 & 0 \\
\hline
 & 1/6 & 1/3 & 1/3 & 1/6
\end{array}$$

Butcher Tableau

RK4 (explicit)

$$\mathbf{u}_{n+1} = \mathbf{u}_n + \Delta t \boxed{\frac{\mathbf{k}_1 + 2\mathbf{k}_2 + 2\mathbf{k}_3 + \mathbf{k}_4}{6}}$$

Estimated slope
(weighted average)

$$\mathbf{k}_1 = f\left(\mathbf{u}_n, t_n\right)$$

Slope at the beginning

$$\mathbf{k}_2 = f\left(\mathbf{u}_n + \mathbf{k}_1 \frac{\Delta t}{2}, t_n + \frac{\Delta t}{2}\right)$$

Slope at the midpoint (k_1 is used to determine the value of u – Euler)

$$\mathbf{k}_3 = f\left(\mathbf{u}_n + \mathbf{k}_2 \frac{\Delta t}{2}, t_n + \frac{\Delta t}{2}\right)$$

Slope at the midpoint (k_2 is now used)

$$\mathbf{k}_4 = f\left(\mathbf{u}_n + \mathbf{k}_3 \Delta t, t_n + \Delta t\right)$$

Slope at the end

RK4 (explicit)

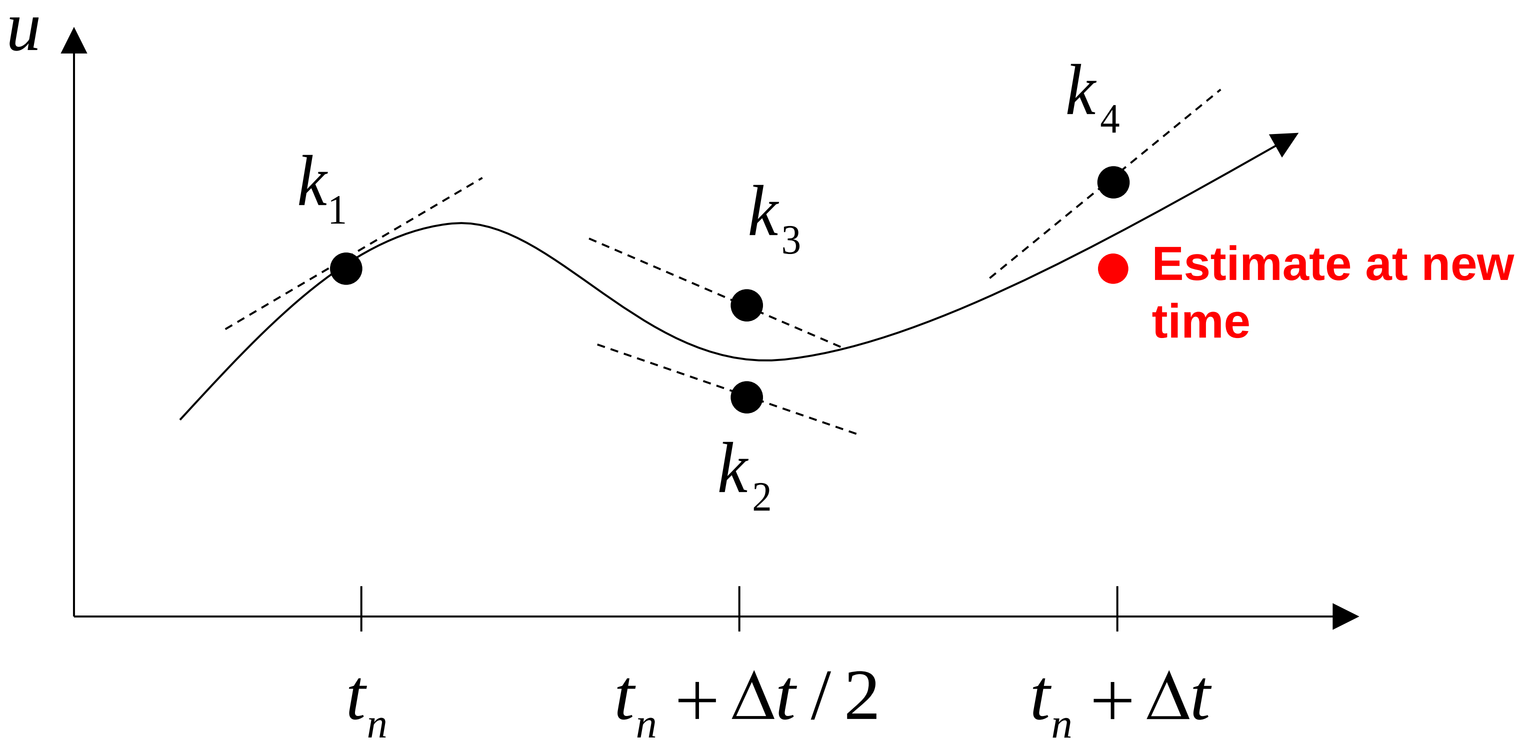

RK4 (explicit)

The local truncation error for a 4^{th} order RK is $O(h^5)$.

The accuracy is comparable to that of a 4^{th} order Taylor series, but the Runge-Kutta method avoids the calculation of higher-order derivatives.

Easy to use and implement.

The step size is fixed.

RK4 in STK

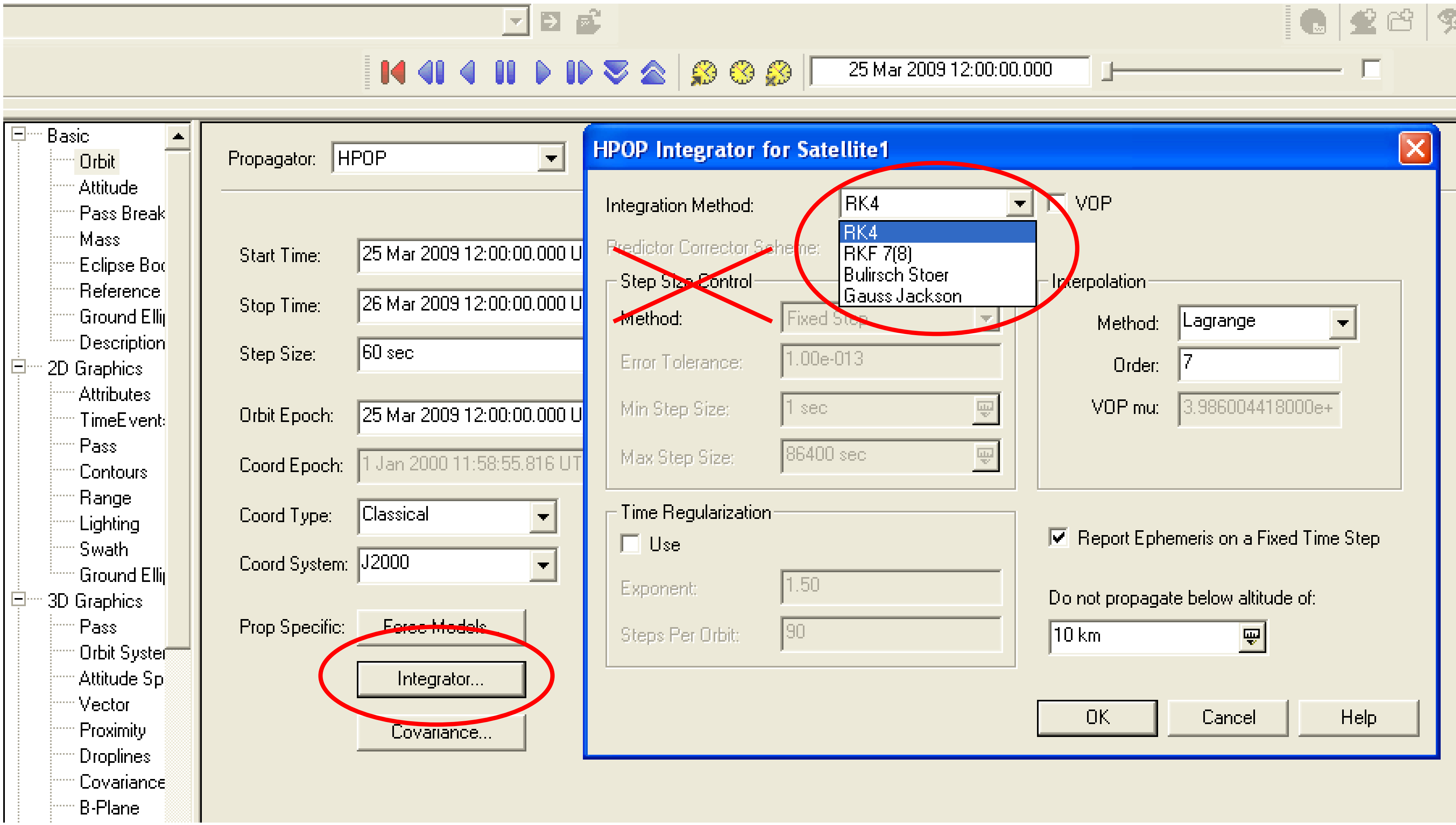
25 Mar 2009 12:00:00.000
Basic
Orbit
Attitude
Pass Break
Mass
Eclipse Bo
Reference
Ground Elli
Description
2D Graphics
Attributes
TimeEvent
Pass
Contours
Range
Lighting
Swath
Ground Elli
3D Graphics
Pass
Orbit Syste
Attitude Sp
Vector
Proximity
Droplines
Covariance
B-Plane
Propagator: HPOP
Start Time: 25 Mar 2009 12:00:00.000 U
Stop Time: 26 Mar 2009 12:00:00.000 U
Step Size: 60 sec
Orbit Epoch: 25 Mar 2009 12:00:00.000 U
Coord Epoch: 1 Jan 2000 11:58:55.816 UT
Coord Type: Classical
Coord System: J2000
Prop Specific: Force Models...
Integrator...
Covariance...
HPOP Integrator for Satellite1
Integration Method: RK4
VOP
RK4
RKF 7(8)
Bulirsch Stoer
Gauss Jackson
Predictor Corrector Scheme:
Step Size Control
Method: Fixed Step
Error Tolerance: 1.00e-013
Min Step Size: 1 sec
Max Step Size: 86400 sec
Interpolation
Method: Lagrange
Order: 7
VOP mu: 3.986004418000e+
Time Regularization
Use
Exponent: 1.50
Steps Per Orbit: 90
Report Ephemeris on a Fixed Time Step
Do not propagate below altitude of:
10 km
OK
Cancel
Help

Embedded methods

They produce an estimate of the local truncation error:

$\Rightarrow$ adjust the step size to keep local truncation errors within some tolerances.

This is done by having two methods in the tableau, one with order p and one with order p+1, with the same set of function evaluations:

$$\mathbf{u}_{n+1}^{(p)} = \mathbf{u}_{n}^{(p)} + \Delta t \sum_{i=1}^{s} b_i^{(p)} \mathbf{k}_i$$

$$\mathbf{u}_{n+1}^{(p+1)} = \mathbf{u}_{n}^{(p+1)} + \Delta t \sum_{i=1}^{s} b_i^{(p+1)} \mathbf{k}_i$$

Embedded methods

The two different approximations for the solution at each step are compared:

If the two answers are in close agreement, the approximation is accepted.

If the two answers do not agree to a specified accuracy, the step size is reduced.

If the answers agree to more significant digits than required, the step size is increased.

Ode45 in Matlab / Simulink

Runge-Kutta (4,5) pair of Dormand and Prince:

$\Rightarrow$ Variable step size.

$\Rightarrow$ Matlab help: *This should be the first solver you try*

0							
1/5	1/5						
3/10	3/40	9/40					
4/5	44/45	−56/15	32/9				
8/9	19372/6561	−25360/2187	64448/6561	−212/729			
1	9017/3168	−355/33	46732/5247	49/176	−5103/18656		
1	35/384	0	500/1113	125/192	−2187/6784	11/84	
	5179/57600	0	7571/16695	393/640	−92097/339200	187/2100	1/40
	35/384	0	500/1113	125/192	−2187/6784	11/84	0

Ode45 in Matlab / Simulink

Editor - C:\Program Files\MATLAB\R2007b\toolbox\matlab\funfun\ode45.m

```
  end
  nout = 1;
  tout(nout) = t;
  yout(:,nout) = y;
end

% Initialize method parameters.
pow = 1/5;
A = [1/5, 3/10, 4/5, 8/9, 1, 1];
B = [
    1/5         3/40    44/45   19372/6561      9017/3168       35/384
    0           9/40    -56/15  -25360/2187     -355/33         0
    0           0       32/9    64448/6561      46732/5247      500/1113
    0           0       0       -212/729        49/176          125/192
    0           0       0       0               -5103/18656     -2187/6784
    0           0       0       0               0               11/84
    0           0       0       0               0               0
    ];
E = [71/57600; 0; -71/16695; 71/1920; -17253/339200; 22/525; -1/40];
f = zeros(neq,7,dataType);
hmin = 16*eps(t);
if isempty(htry)
  % Compute an initial step size h using y'(t).
  absh = min(hmax, htspan);
```

edit ode45

Ode45 in Matlab / Simulink

Be very careful with the default parameters !

```
options = odeset('RelTol',1e-8,'AbsTol',1e-8);
```

RKF 7(8): default method in STK

Runge-Kutta-Fehlberg integration method of 7th order with 8th order error control for the integration step size.

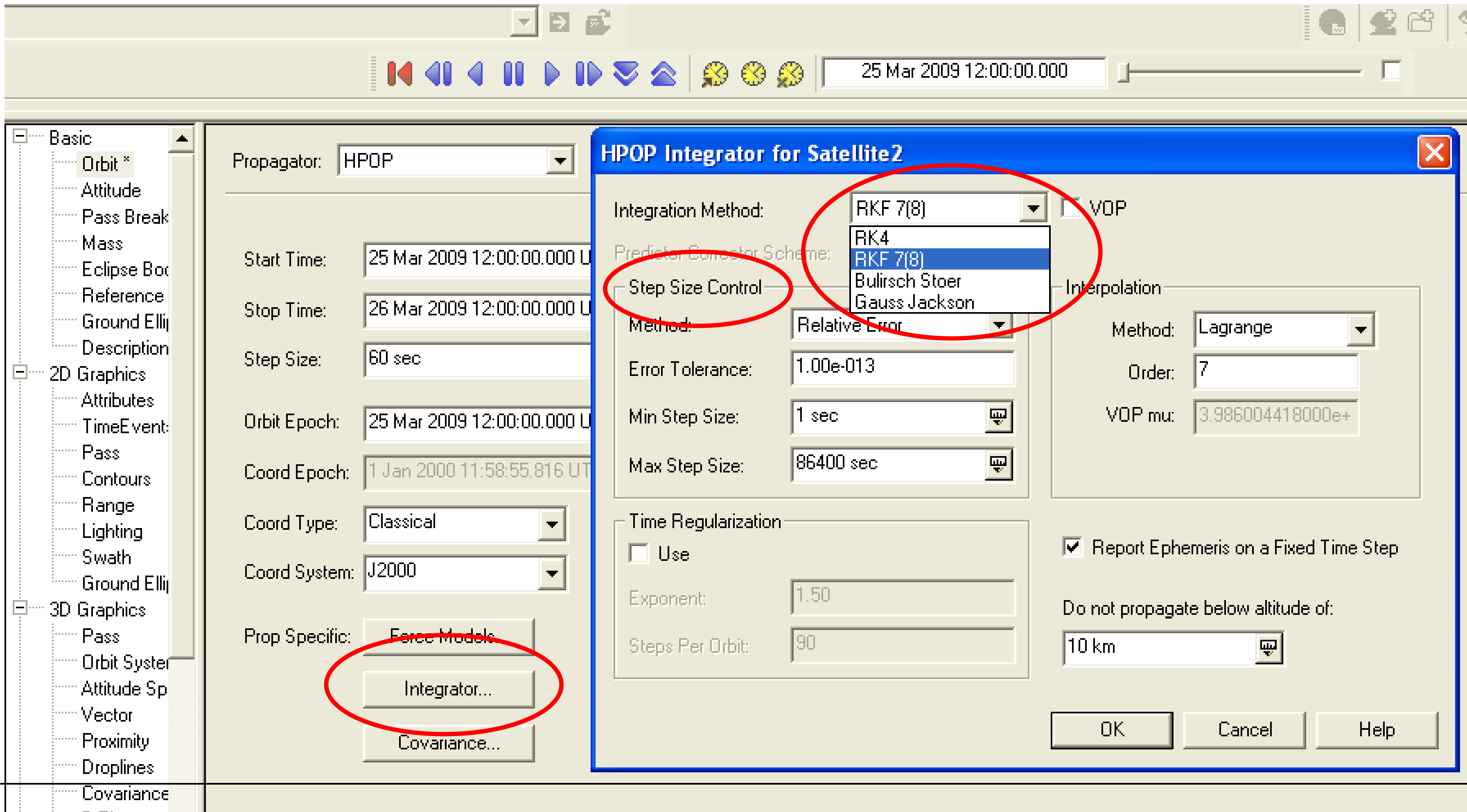

Table 5.3. Fehlberg 7(8)

0													
$\frac{2}{27}$	$\frac{2}{27}$												
$\frac{1}{9}$	$\frac{1}{36}$	$\frac{1}{12}$											
$\frac{1}{6}$	$\frac{1}{24}$	0	$\frac{1}{8}$										
$\frac{5}{12}$	$\frac{5}{12}$	0	$-\frac{25}{16}$	$\frac{25}{16}$									
$\frac{1}{2}$	$\frac{1}{20}$	0	0	$\frac{1}{4}$	$\frac{1}{5}$								
$\frac{5}{6}$	$-\frac{25}{108}$	0	0	$\frac{125}{108}$	$-\frac{65}{27}$	$\frac{125}{54}$							
$\frac{1}{6}$	$\frac{31}{300}$	0	0	0	$\frac{61}{225}$	$-\frac{2}{9}$	$\frac{13}{900}$						
$\frac{2}{3}$	2	0	0	$-\frac{53}{6}$	$\frac{704}{45}$	$-\frac{107}{9}$	$\frac{67}{90}$	3					
$\frac{1}{3}$	$-\frac{91}{108}$	0	0	$\frac{23}{108}$	$-\frac{976}{135}$	$\frac{311}{54}$	$-\frac{19}{60}$	$\frac{17}{6}$	$-\frac{1}{12}$				
1	$\frac{2383}{4100}$	0	0	$-\frac{341}{164}$	$\frac{4496}{1025}$	$-\frac{301}{82}$	$\frac{2133}{4100}$	$\frac{45}{82}$	$\frac{45}{164}$	$\frac{18}{41}$			
0	$\frac{3}{205}$	0	0	0	0	$-\frac{6}{41}$	$-\frac{3}{205}$	$-\frac{3}{41}$	$\frac{3}{41}$	$\frac{6}{41}$	0		
1	$-\frac{1777}{4100}$	0	0	$-\frac{341}{164}$	$\frac{4496}{1025}$	$-\frac{289}{82}$	$\frac{2193}{4100}$	$\frac{51}{82}$	$\frac{33}{164}$	$\frac{12}{41}$	0	1	
y_1	$\frac{41}{840}$	0	0	0	0	$\frac{34}{105}$	$\frac{9}{35}$	$\frac{9}{35}$	$\frac{9}{280}$	$\frac{9}{280}$	$\frac{41}{840}$	0	0
$\widehat{y}_1$	0	0	0	0	0	$\frac{34}{105}$	$\frac{9}{35}$	$\frac{9}{35}$	$\frac{9}{280}$	$\frac{9}{280}$	0	$\frac{41}{840}$	$\frac{41}{840}$

Integrator selection

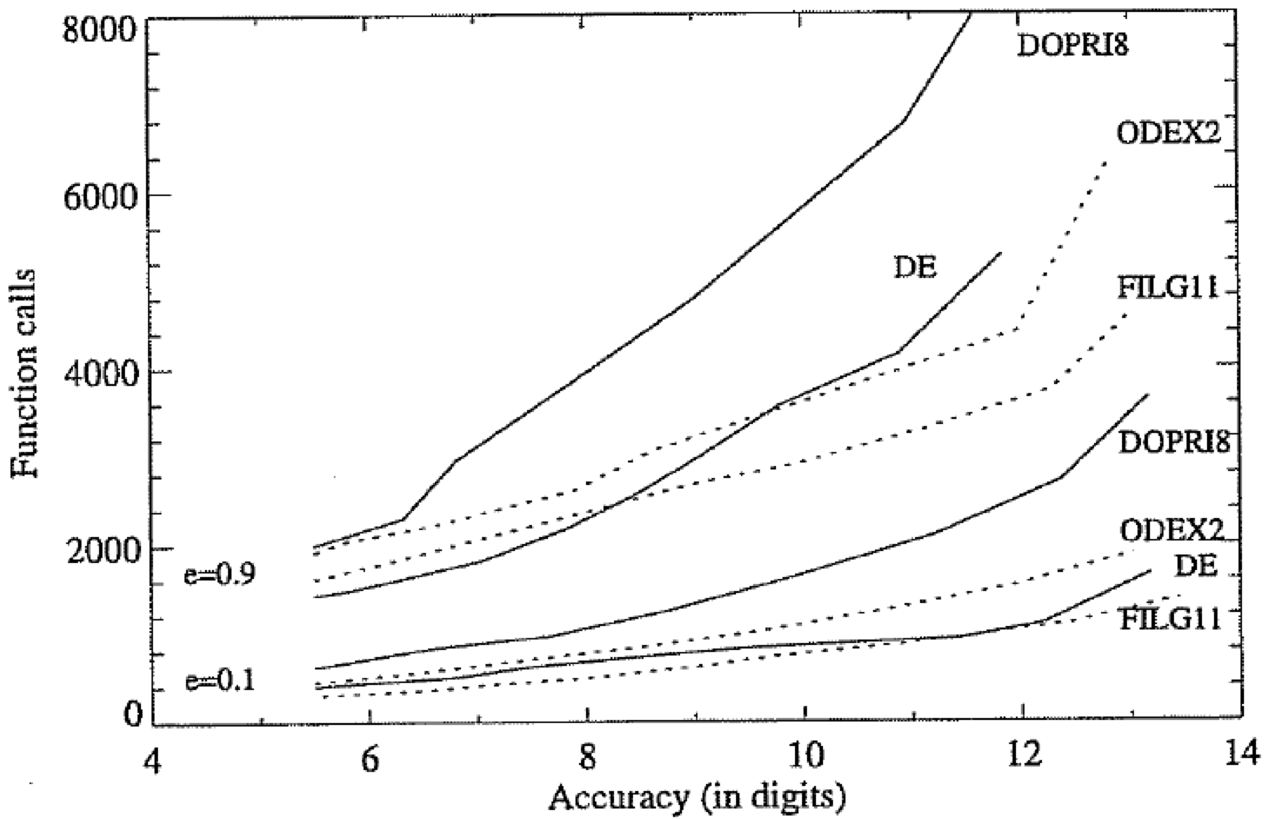

Montenbruck and Gill, *Satellite orbits,* Springer, 2000

Fig. 4.9. Performance diagram of several single- and multistep methods for test cases D1 (e=0.1, lower set of curves) and D5 (e=0.9, upper set of curves) of Hull et al. (1972). The number of function calls is plotted versus the relative accuracy in digits.

Why is the step size so critical ?

Theoretical arguments:

1. The accuracy and the stability of the algorithm are directly related to the step size.
2. Nonlinear equations of motion.

Data for Landsat 4 and 6 in circular orbits around 800km indicates that a one-minute step size yields about 47m error.

A three-minute step size produces about a 900m error !

Why is the step size so critical ?

More practical arguments:

1. The computation time is directly related to the step size.

2. The particular choice of step size depends on the most rapidly varying component in the disturbing functions (e.g., 50 x 50 gravity field).

XMM (e~0.8)

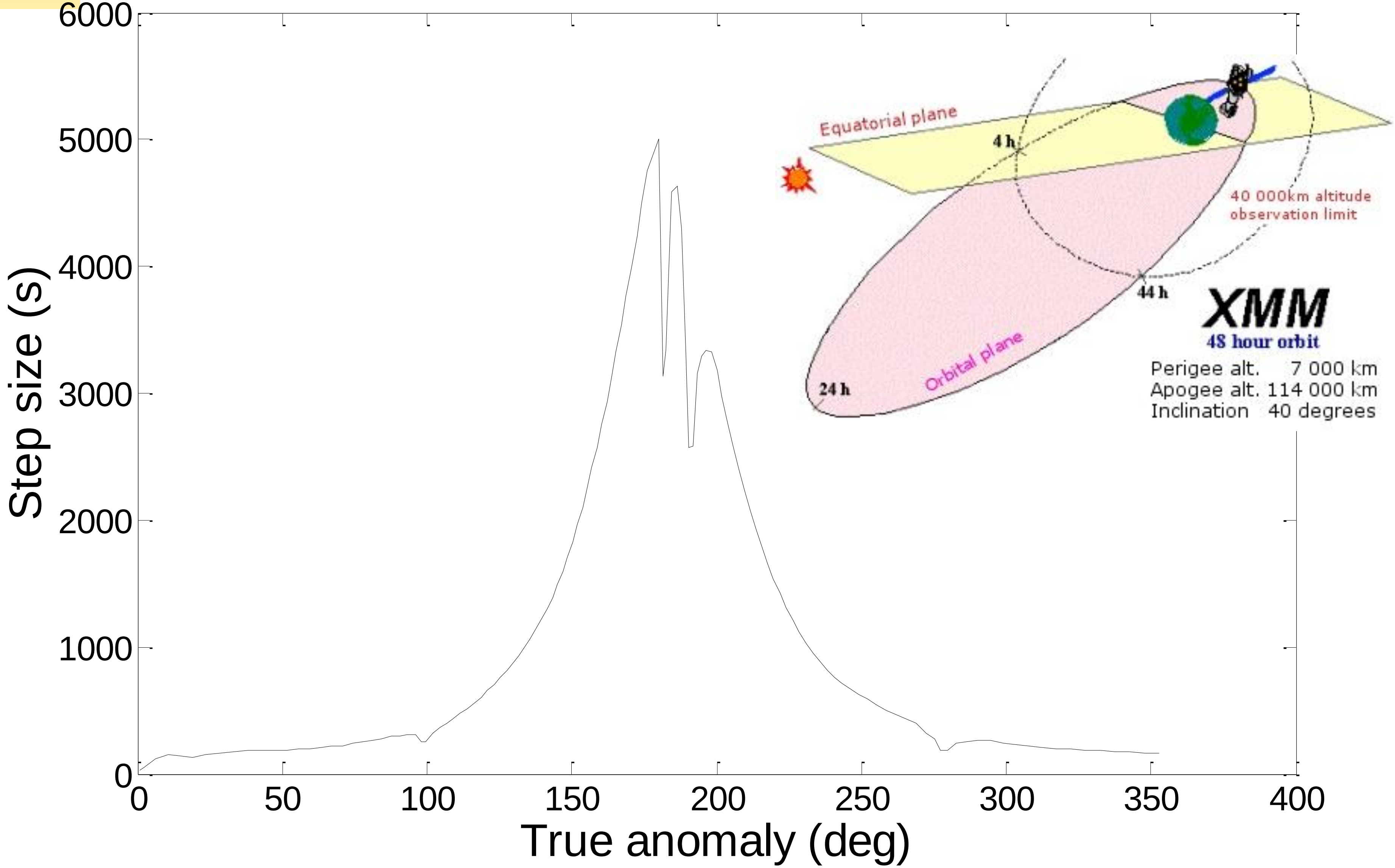

6000
5000
4000
3000
2000
1000
0
0
50
100
150
200
250
300
350
400
Step size (s)
True anomaly (deg)
Equatorial plane
4 h
40 000km altitude
observation limit
44 h
XMM
48 hour orbit
Perigee alt. 7 000 km
Apogee alt. 114 000 km
Inclination 40 degrees
Orbital plane
24 h

ISS(e~0)

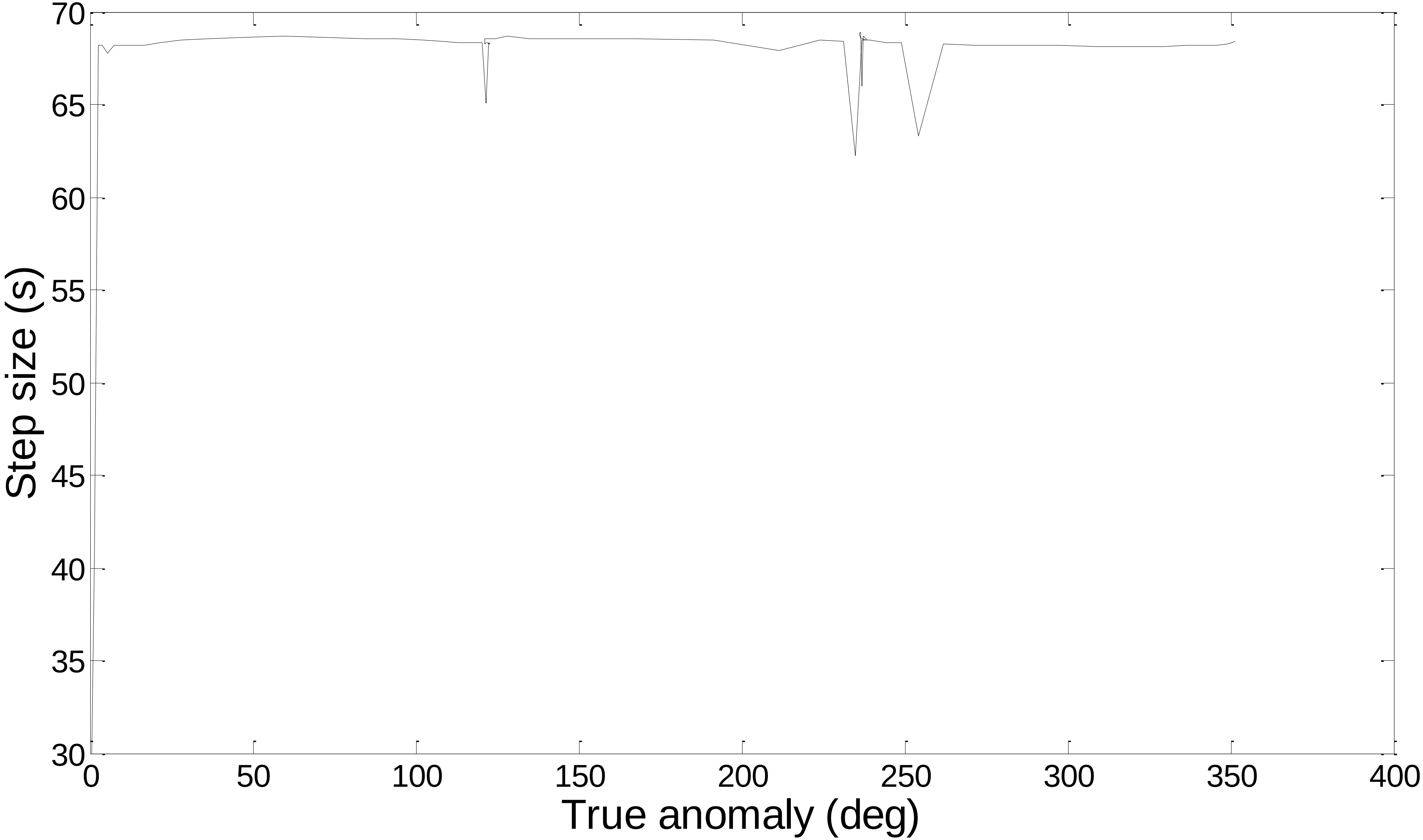
70
65
60
55
50
45
40
35
30
Step size (s)
0
50
100
150
200
250
300
350
400
True anomaly (deg)

“Difficult” orbits

Automatic time step is especially nice on highly eccentric orbits (Molniya, XMM). These orbits are best computed using variable step sizes to maintain some given level of accuracy:

> Without this variable step size, we waste a lot of time near apoapsis, when the integration is taking too small a step.
>
> Likewise, the integrator may not be using a small enough step size at periapsis, where the satellite is traveling fast.

Orbital propagation

$$\dot{\Omega} = \sqrt{\frac{a(1-e^2)}{\mu}} \frac{N \sin\theta_2}{\sin i\left(1+e\cos\theta\right)}$$

Analytic treatment

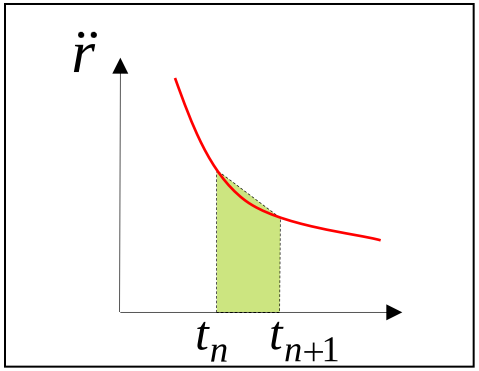

Numerical methods

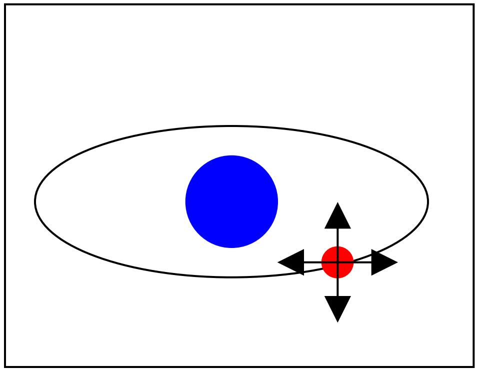

ISS and geostationary satellites

ISS example

1. Earth's oblateness only
2. Drag only
3. Sun and moon only
4. SRP only
5. All together.

J2 only

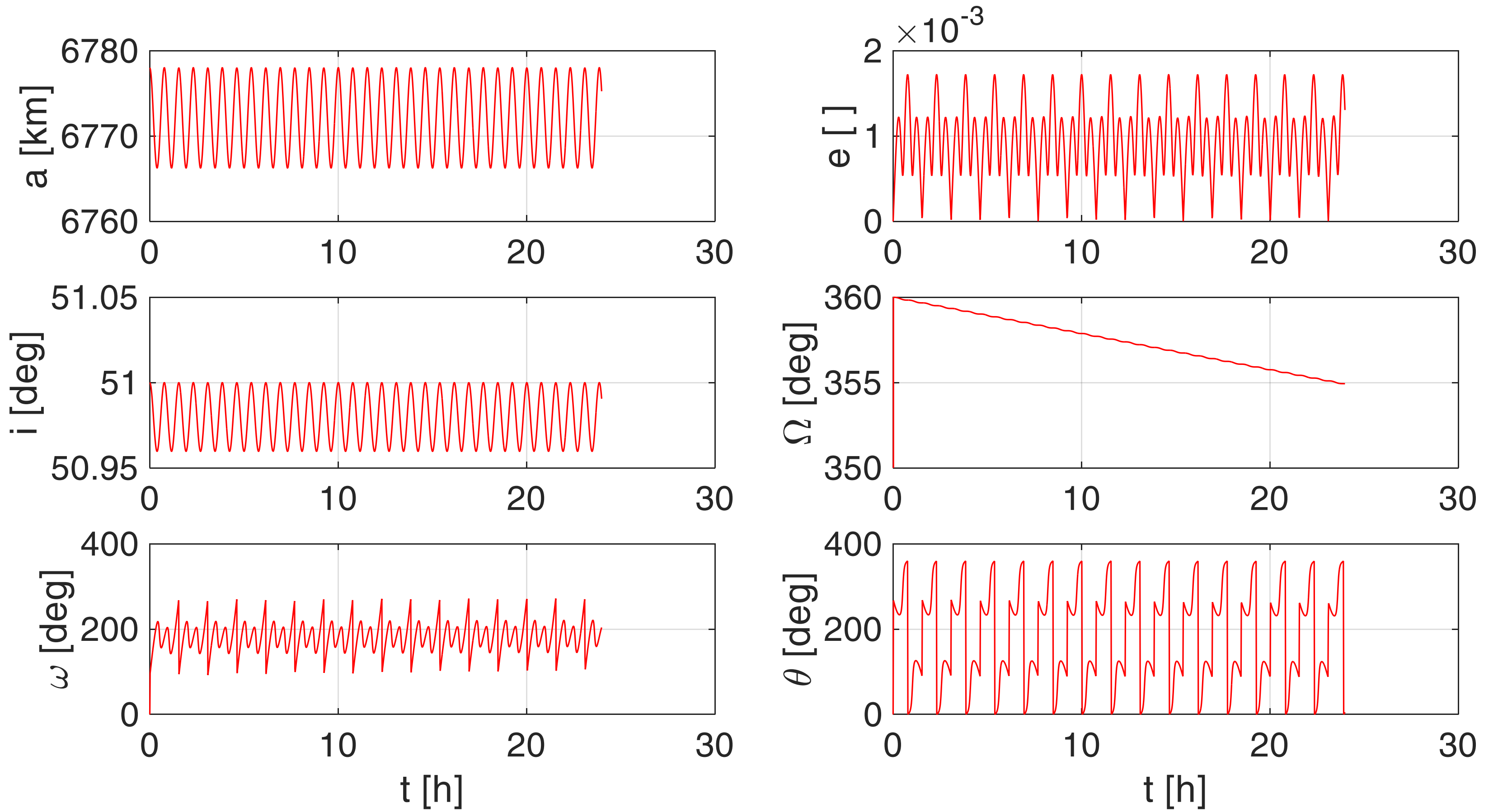

a [km]
6780
6770
6760
e [ ]
×10^-3
2
1
0
i [deg]
51.05
51
50.95
Ω [deg]
360
355
350
ω [deg]
400
200
0
θ [deg]
400
200
0
0
10
20
30
t [h]
t [h]

Overall effects of the J2 perturbation

Nodal regression: regression of the nodal line:

$$\dot{\Omega}_{avg} = \frac{1}{T}\int_0^T \dot{\Omega}\,dt = -\left[\frac{3}{2}\frac{\sqrt{\mu}J_2R^2}{(1-e^2)^2a^{7/2}}\right]\cos i$$

Apsidal rotation: rotation of the apse line:

$$\dot{\omega}_{avg} = \frac{1}{T}\int_0^T \dot{\omega}\,dt = \left[\frac{3}{4}\frac{\sqrt{\mu}J_2R^2}{(1-e^2)^2a^{7/2}}\right]\left(4-5\sin^2 i\right)$$

Mean anomaly.

No secular variations for *a*, *e*, *i* because we have a conservative perturbation.

Drag only: i, Ω, a

HPOP with drag – Harris Priester
(without oblateness/SRP/Sun and Moon)

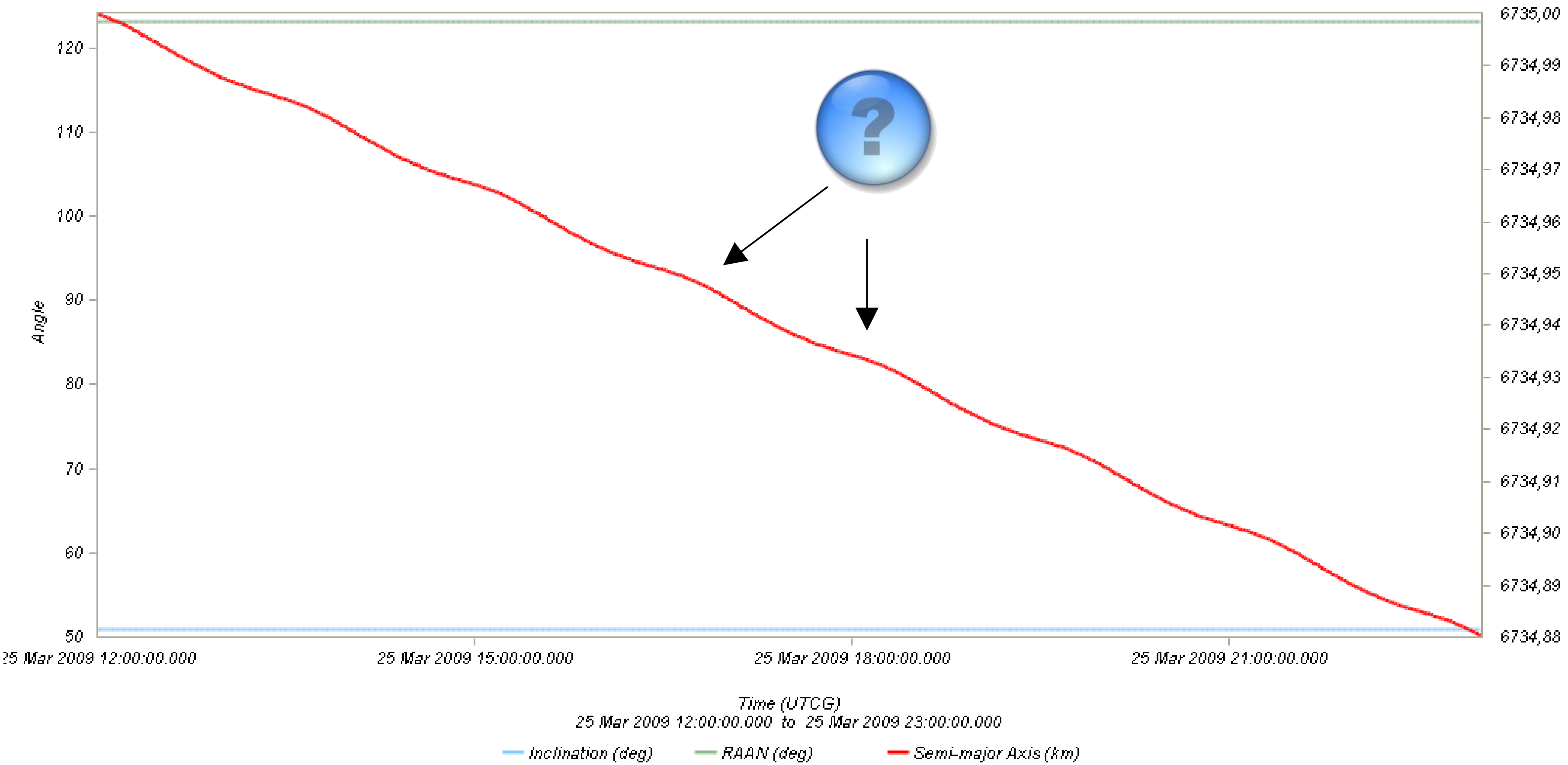

Drag: relationship with eclipses

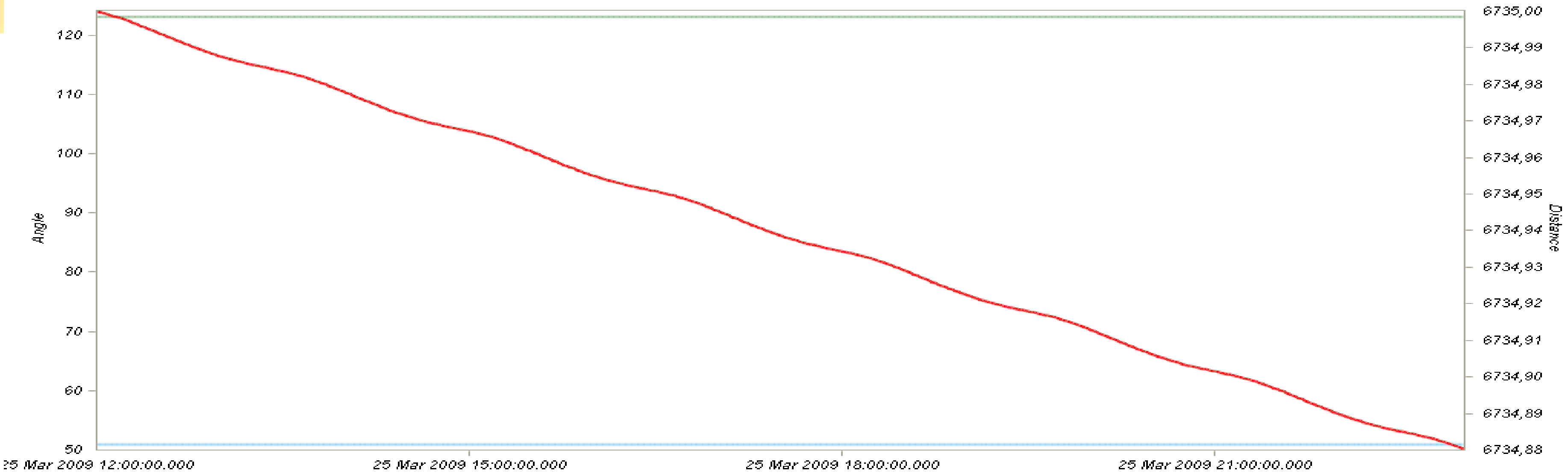

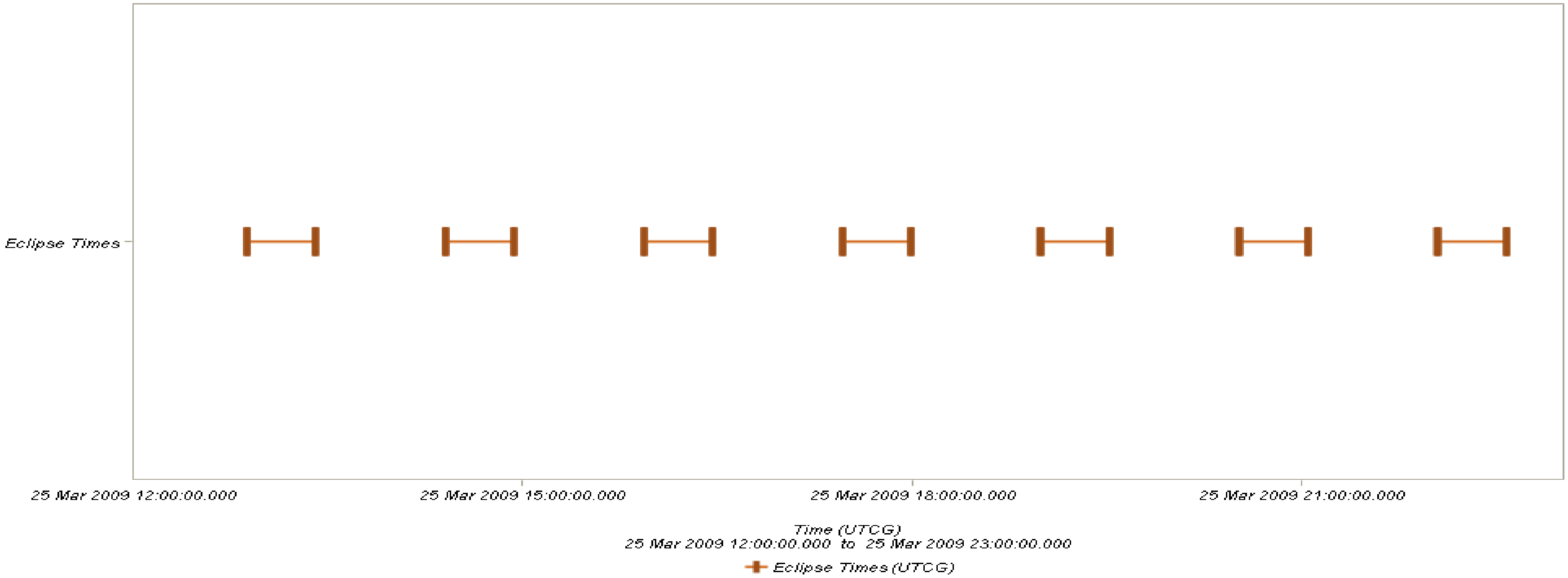

SRP only: i, Ω, a

HPOP with SRP
(without oblateness/drag/Sun and Moon)

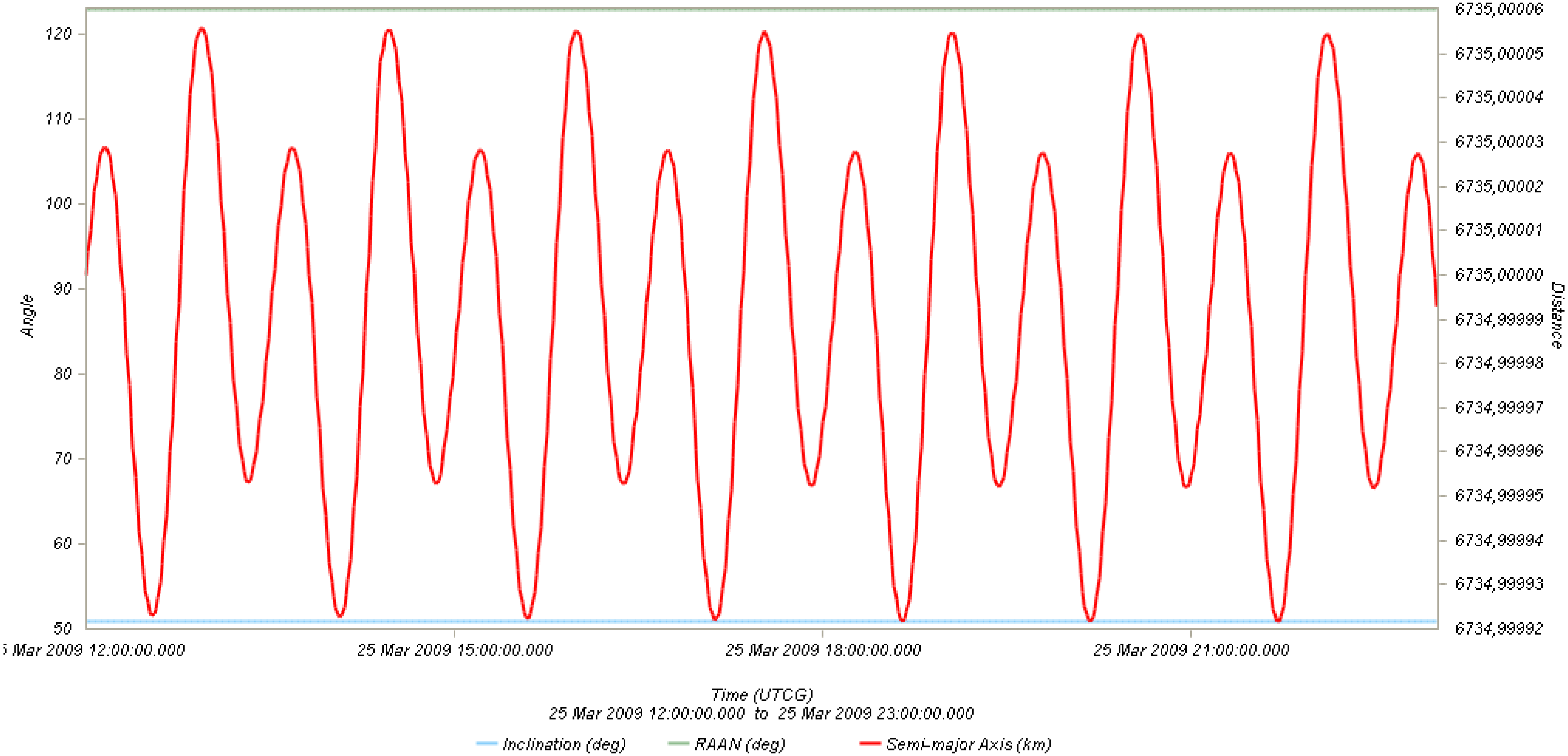

SRP: relationship with eclipses

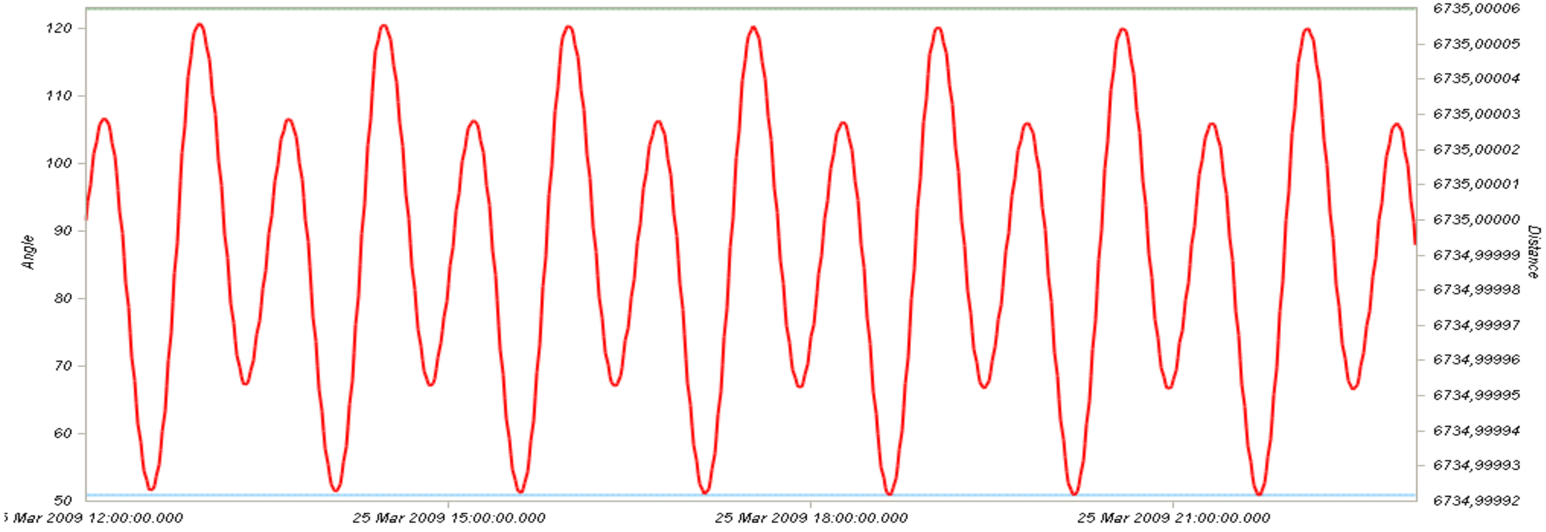

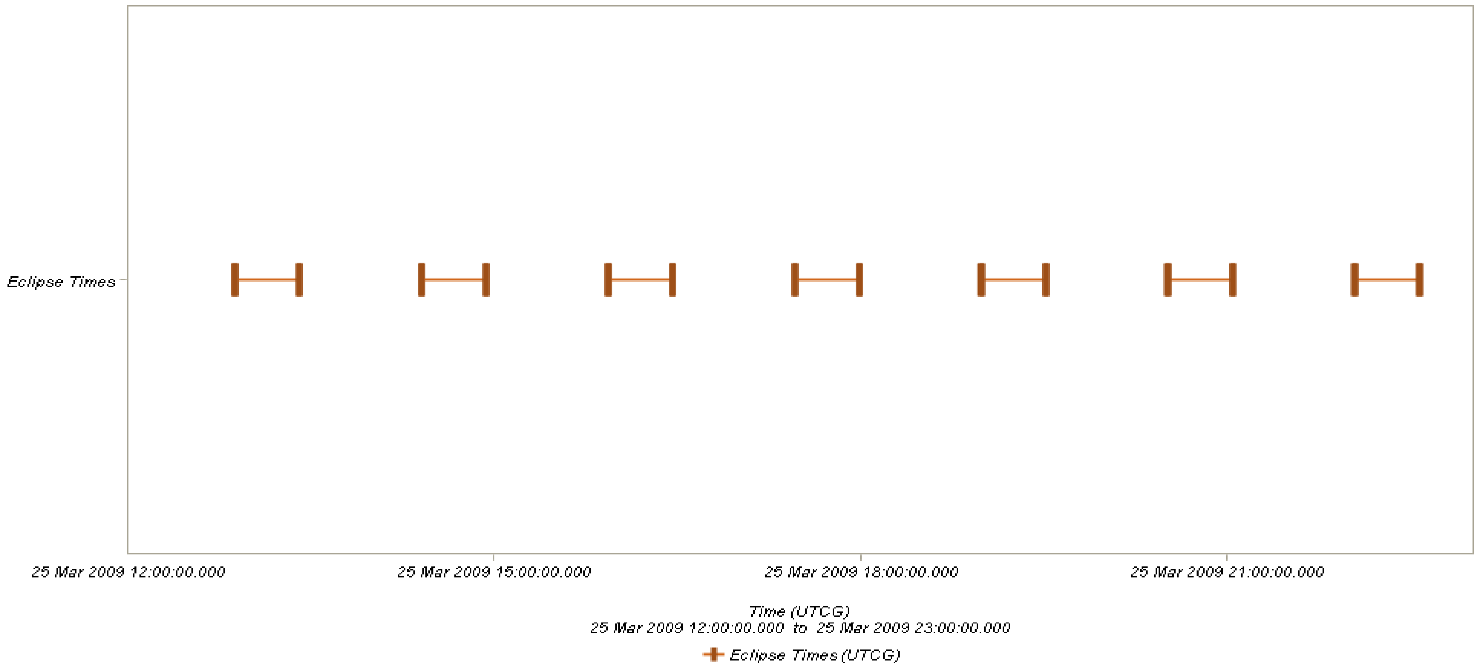

All perturbations together

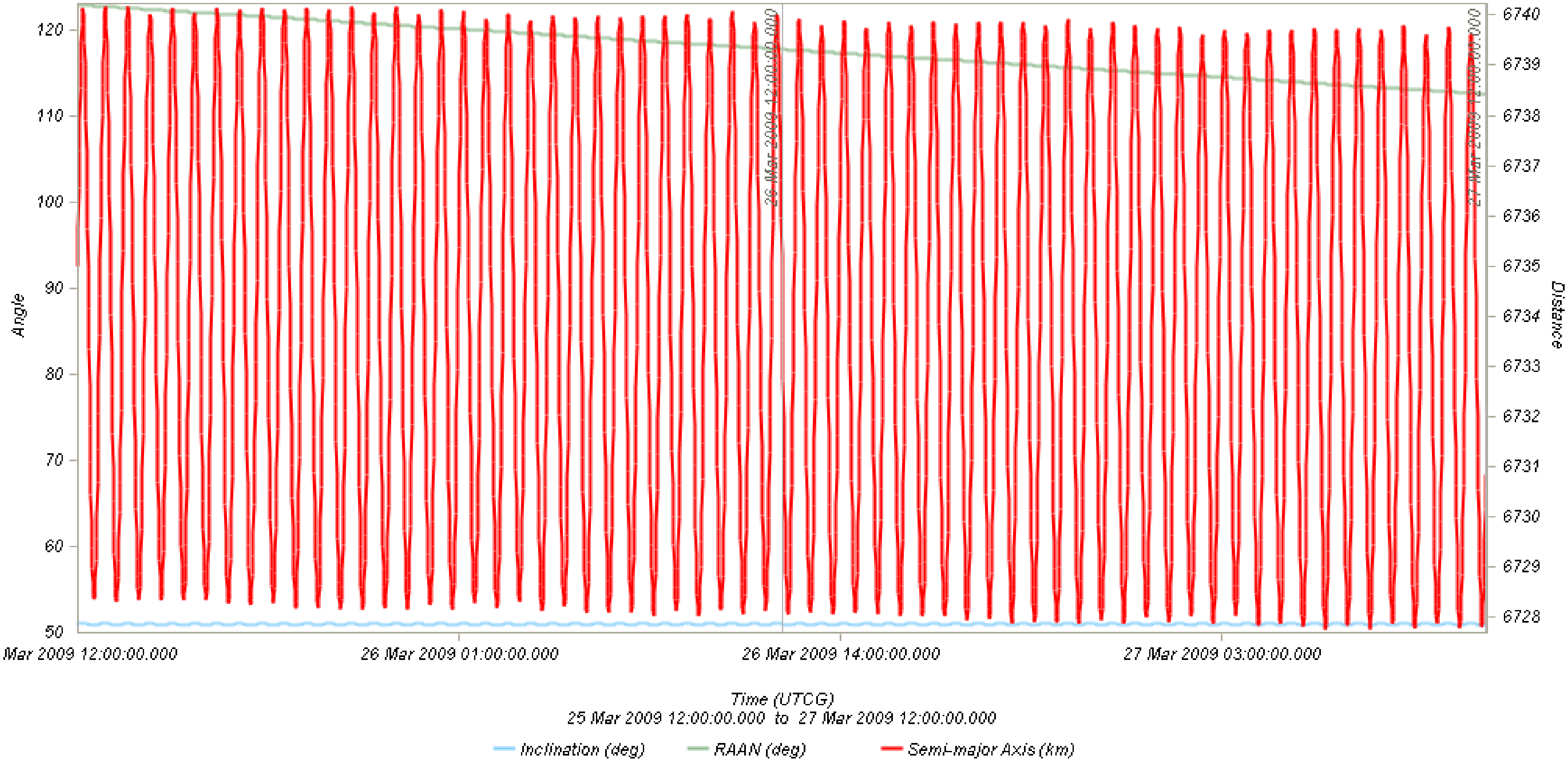

GEO Satellites

Nice illustration of:

1. Perturbations of the 2-body problem.
2. Secular and periodic contributions.
3. Accuracy required by practical applications.
4. The need for orbit correction and thrust forces.

And it is a real-life example (telecommunications, meteorology) !

Three main perturbations for GEO satellites

1. Non-spherical Earth

2. SRP

3. Sun and Moon

Station keeping of GEO satellites

The effect of the perturbations is to cause the spacecraft to drift away from its nominal station. If the drift was allowed to build up unchecked, the spacecraft could become useless.

A station-keeping box is defined by a longitude and a maximum authorized distance for satellite excursions in longitude and latitude.

For instance, TC2: $-8^{\circ} \pm 0.07^{\circ}$ E/W $\pm 0.05^{\circ}$ N/S

East-West and North-South drift

What are the perturbations generating these drifts ?

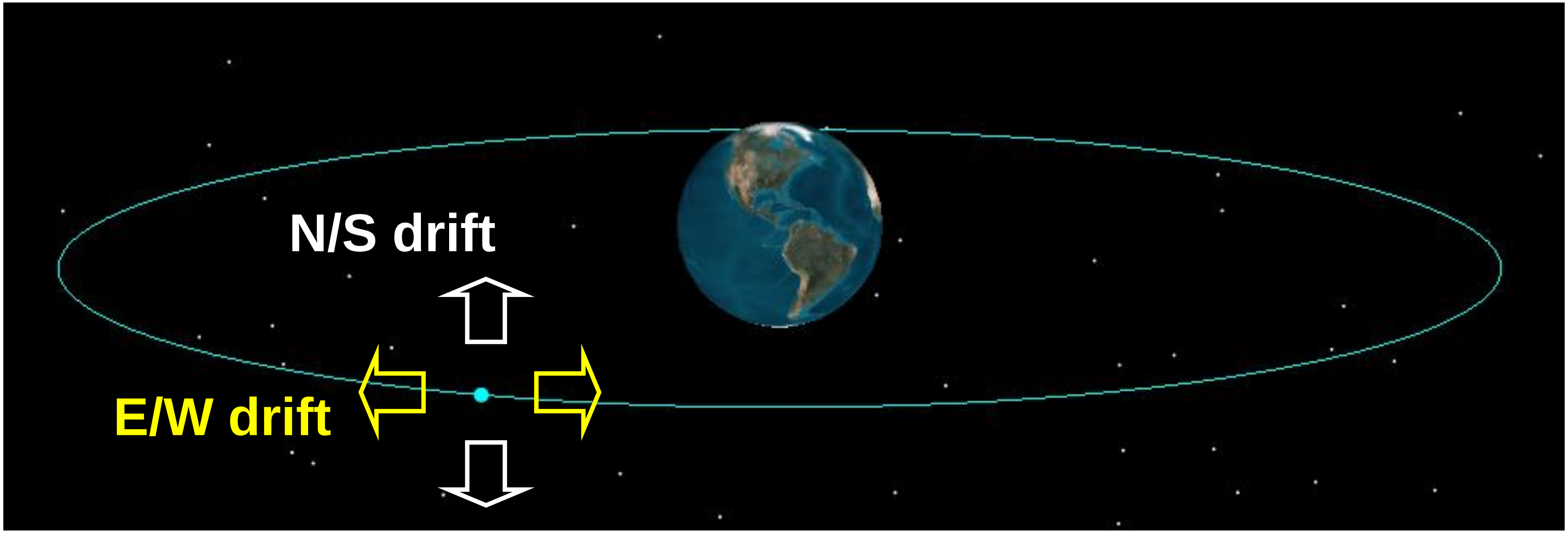

East-West drift

A GEO satellite drifts in longitude due to the influence of two main perturbations:

1. The elliptic nature of the Earth's equatorial cross-section: J22 (and not from the N/S oblateness J2).

2.

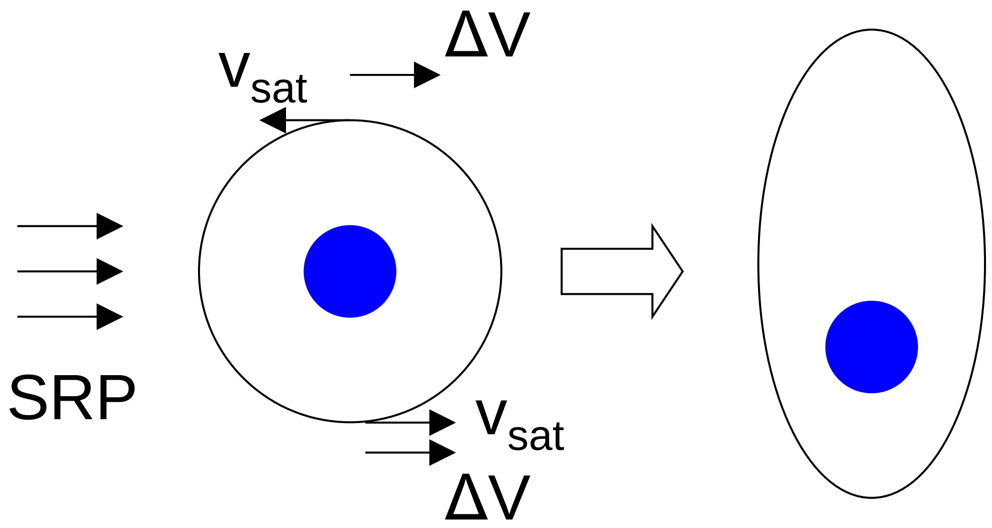

East-West drift due to equatorial ellipticity

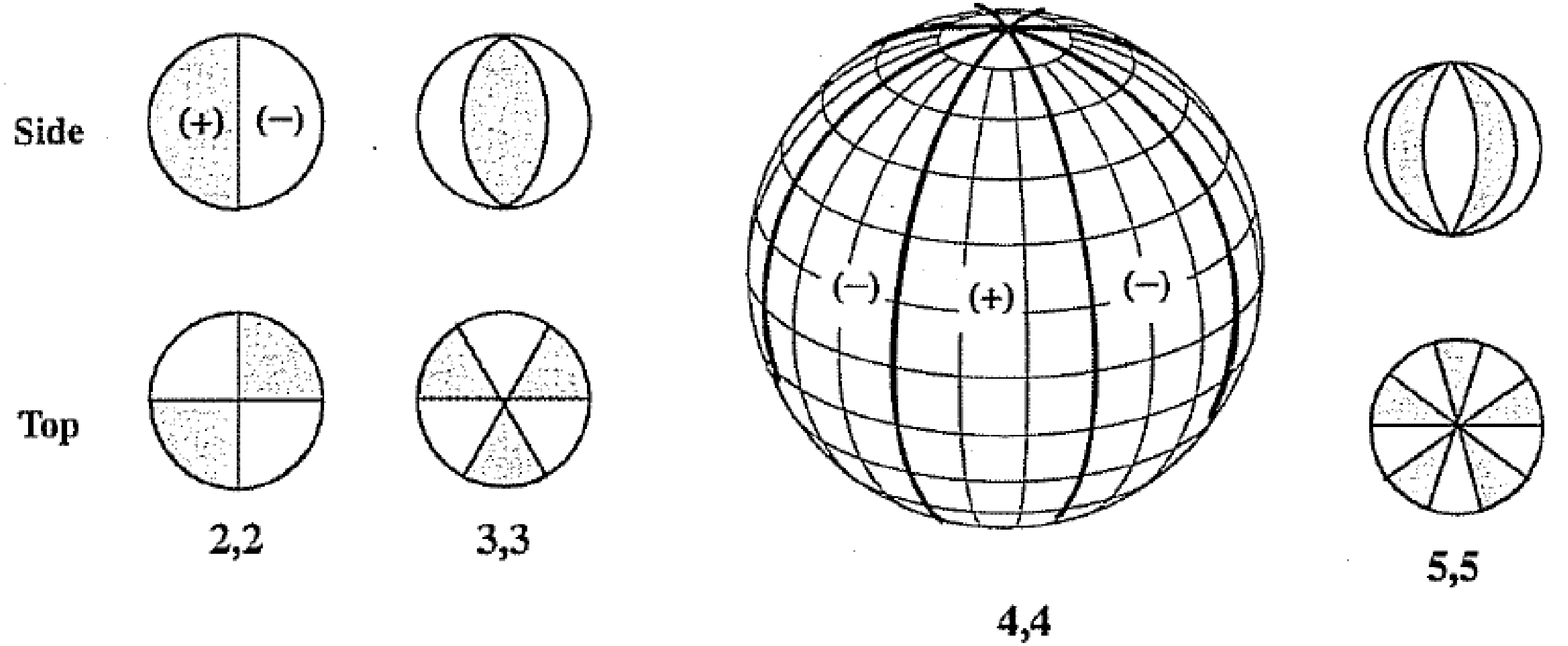

Figure 8-5. Sectorial Harmonics. Sectorial harmonics take into account the extra mass distribution in longitudinal regions.

East-West drift due to equatorial ellipticity

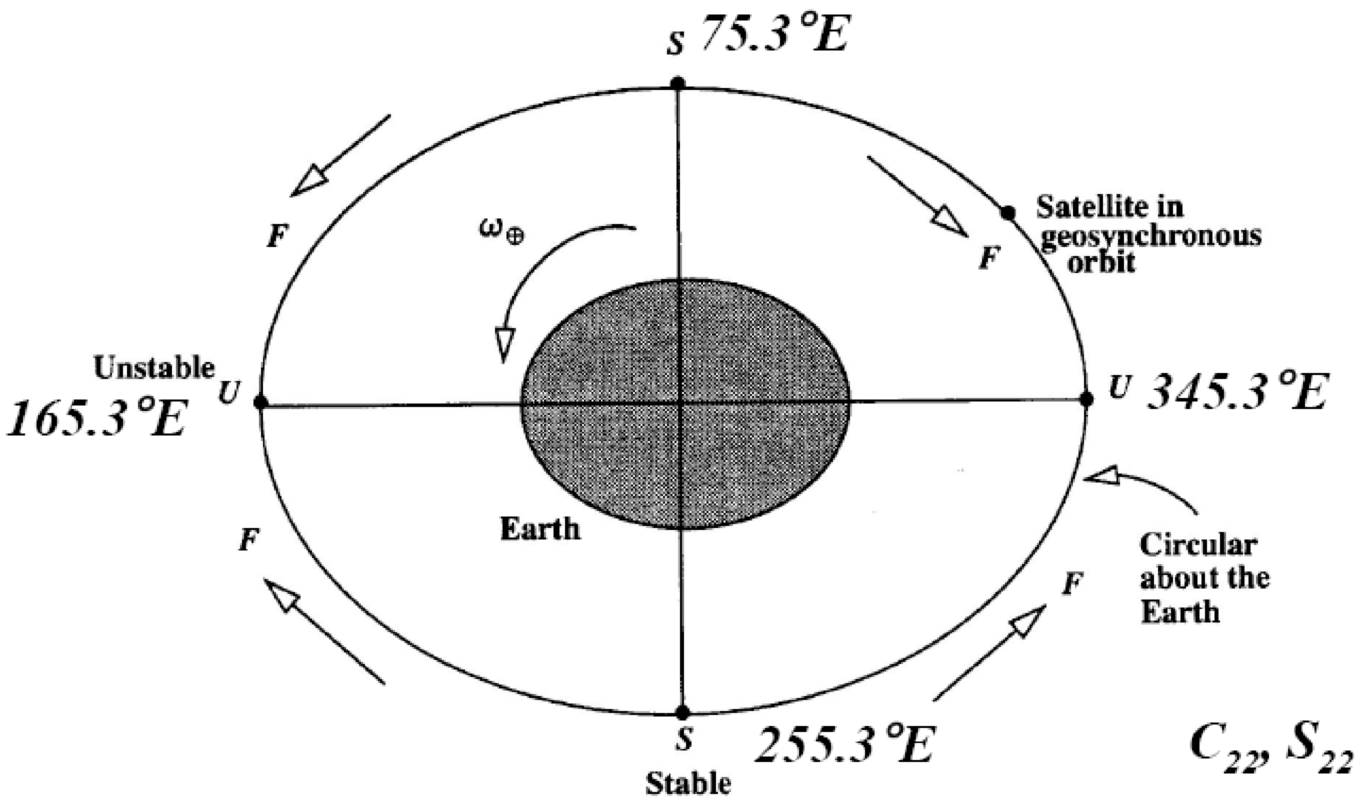

Figure 8-8. Polar View of an Equatorial Section of the Earth. (C_{22} only) F is the net tangential force on the satellite at the positions shown. C_{22} models a longitudinal asymmetry of the Earth. Both stable (S) and unstable (U) positions are identified.

(Vallado, 1997)

East-West drift: stable equilibirum

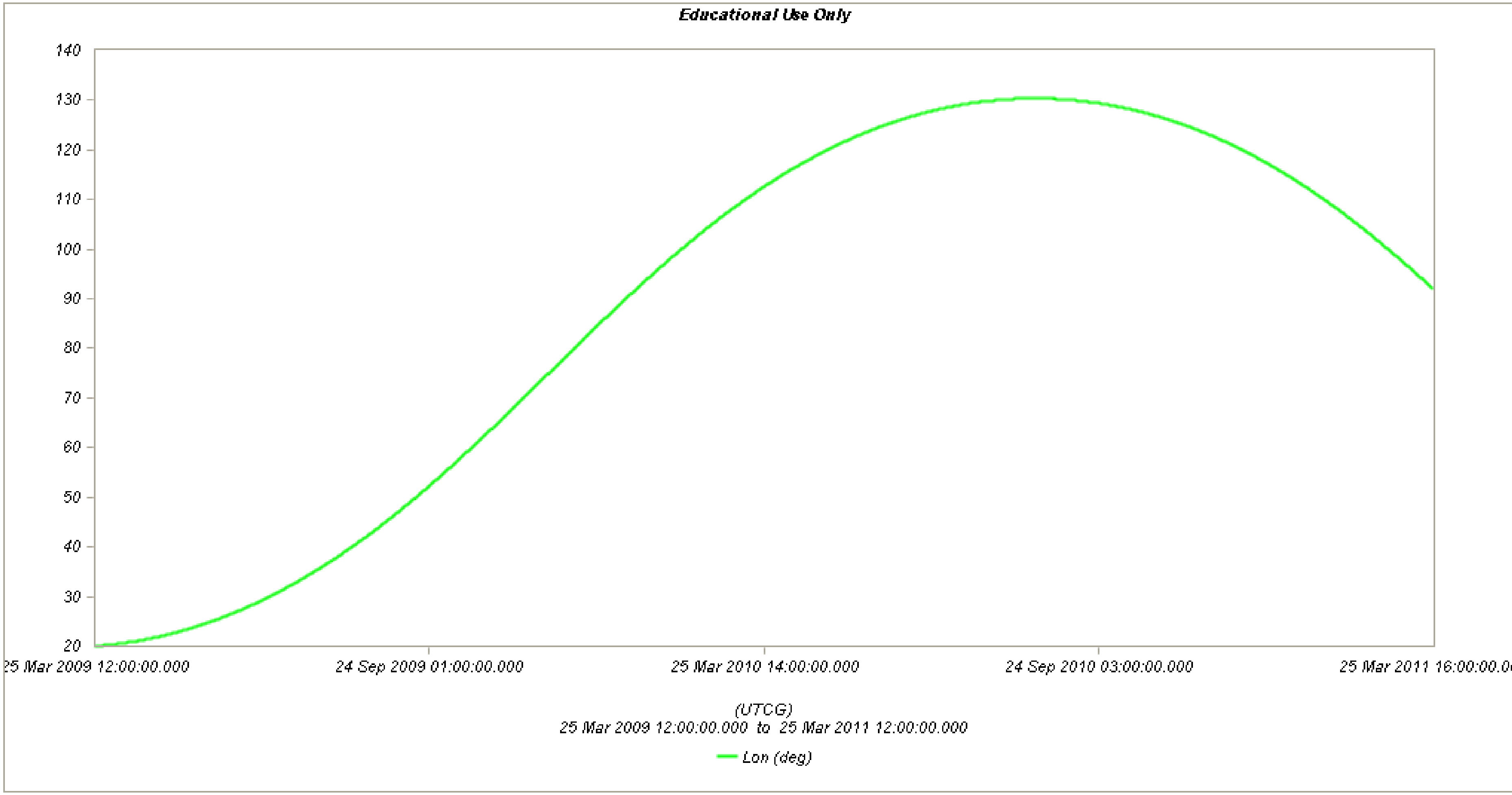

HPOP with 2,2

(without Sun and moon/SRP/drag)

East-West drift: stable equilibirum

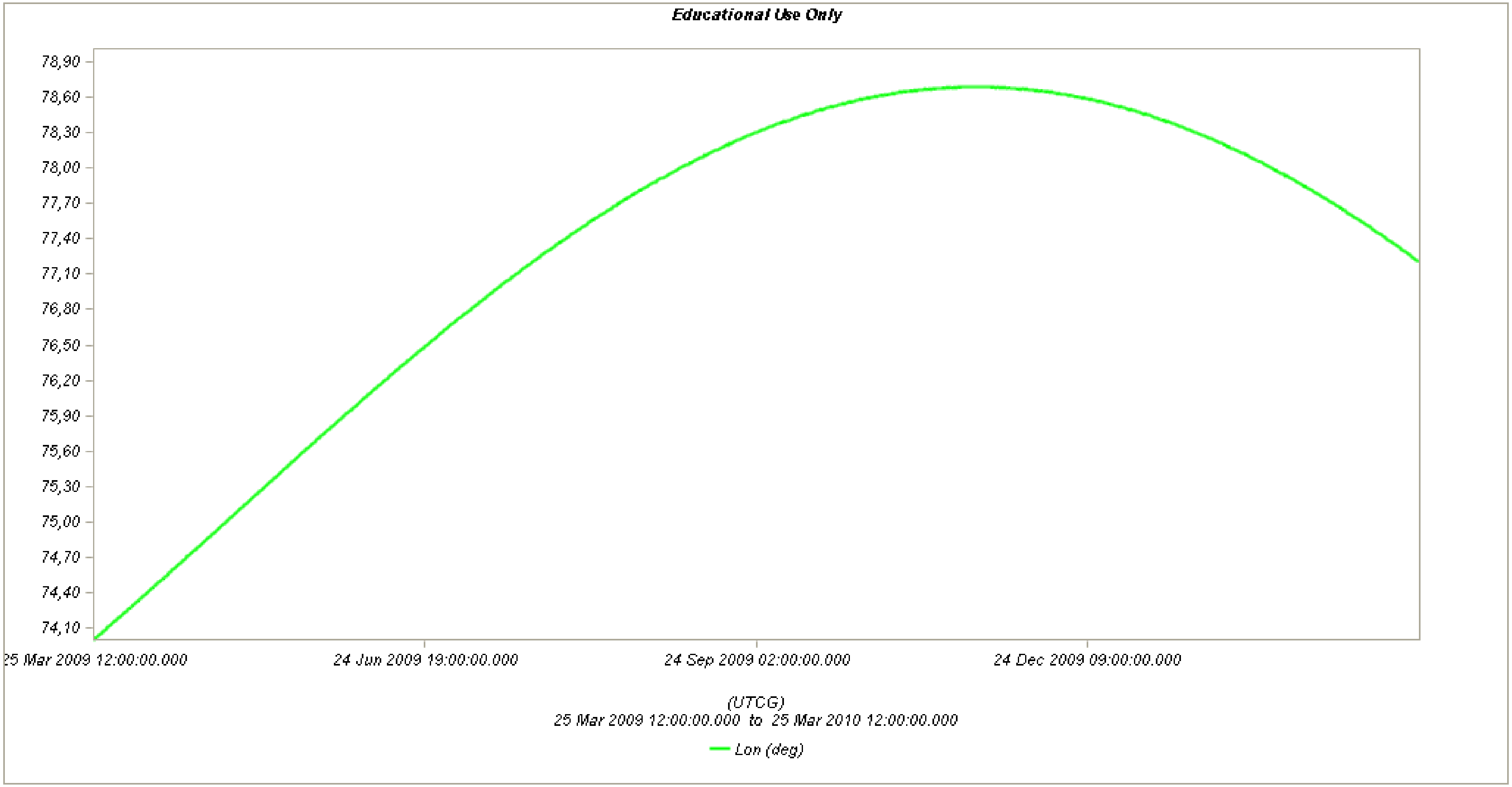

HPOP with 2,2
(without Sun and moon/SRP/drag)

East-West drift: stable equilibirum

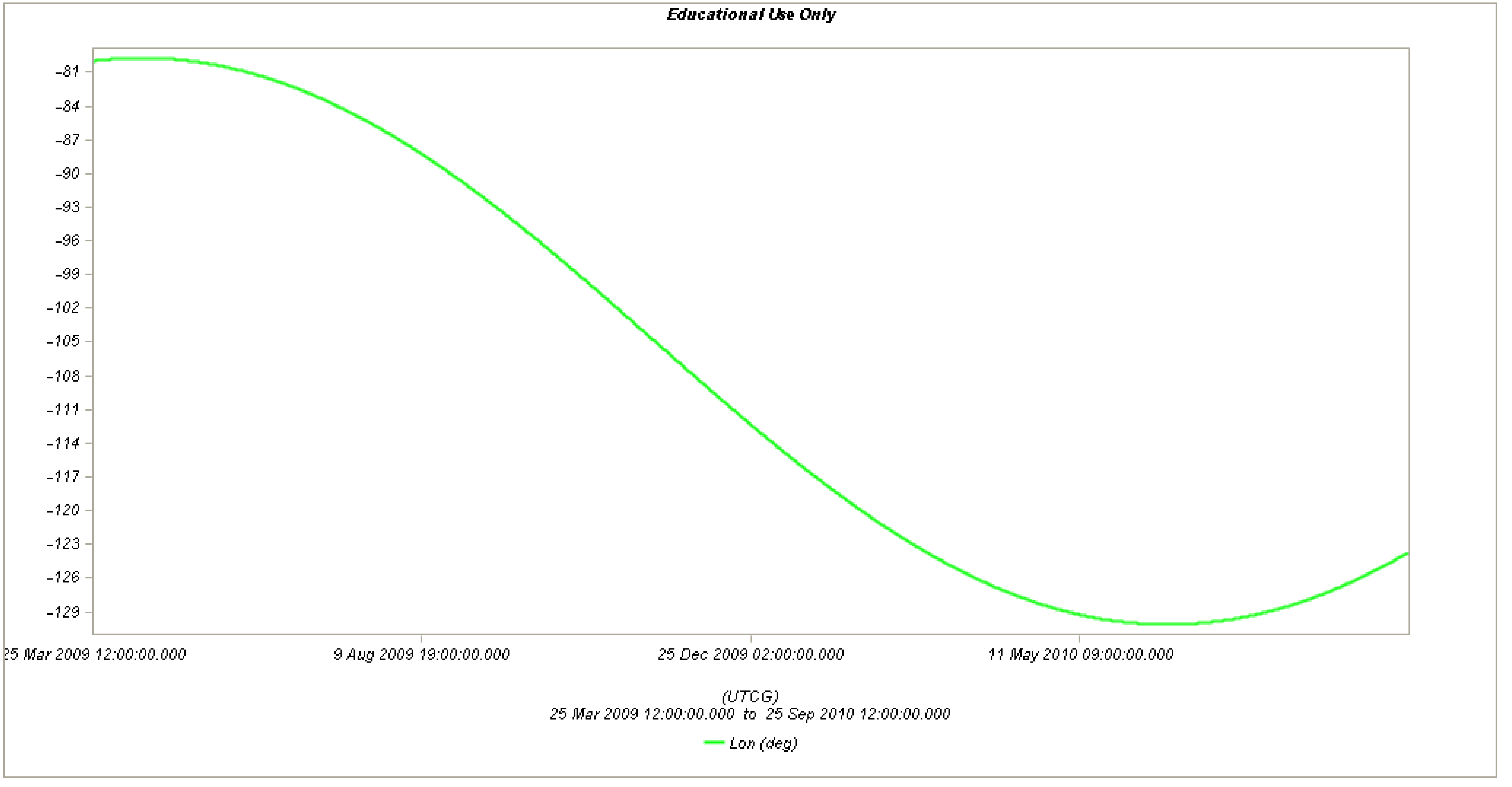

HPOP with 2,2
(without Sun and moon/SRP/drag)

North-South drift

The perturbations caused by the Sun and the Moon are predominantly out-of-plane effects causing a change in the inclination and in the right ascension of the orbit ascending node.

Similar effects on the orbit to those of the Earth’s oblateness (but here with respect to the ecliptic)

A GEO satellite therefore drifts in latitude with a fundamental period equal to the orbit period.

North-South drift

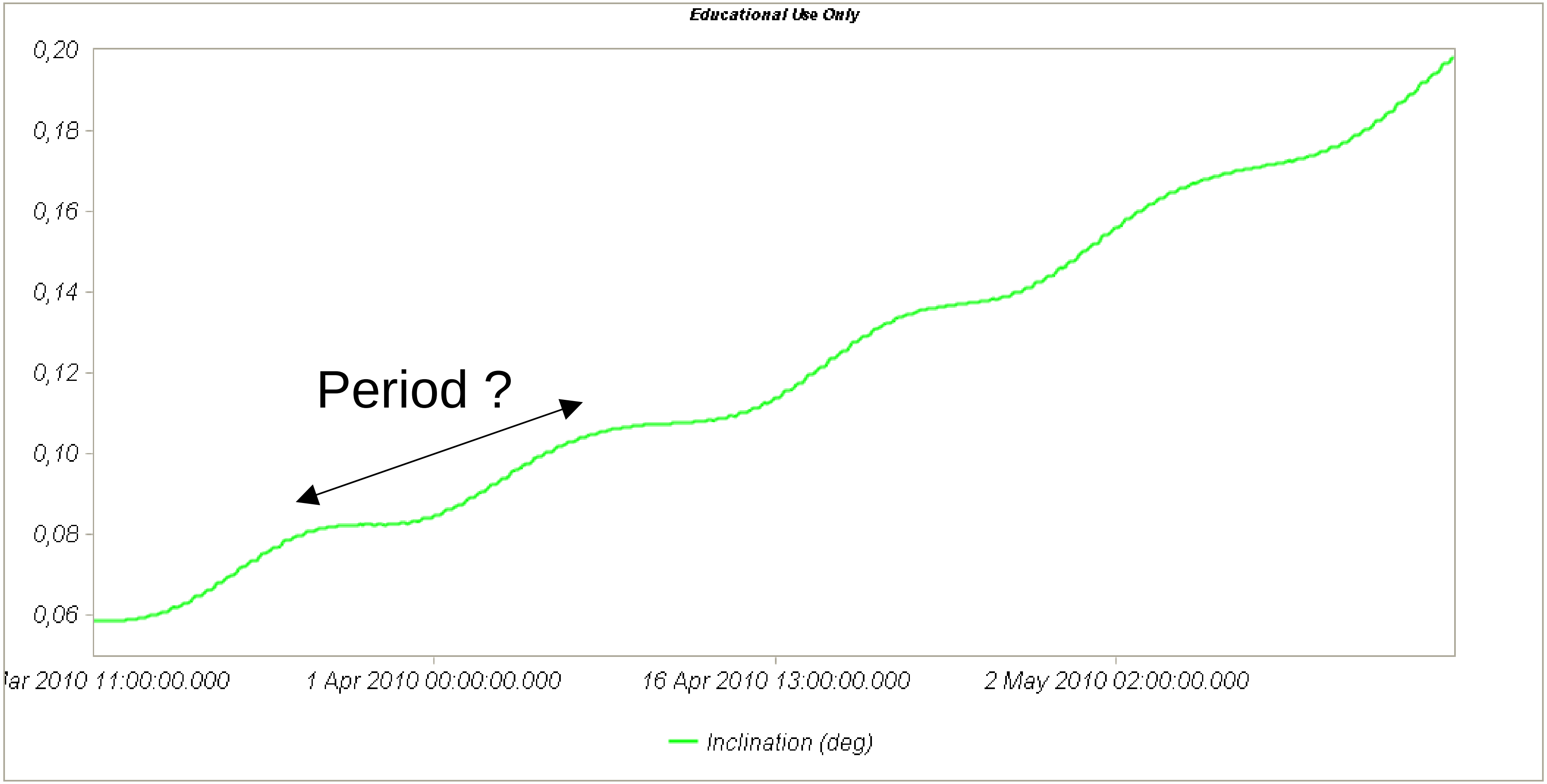

HPOP with Sun and Moon
(without oblateness/SRP/drag)

North-South drift

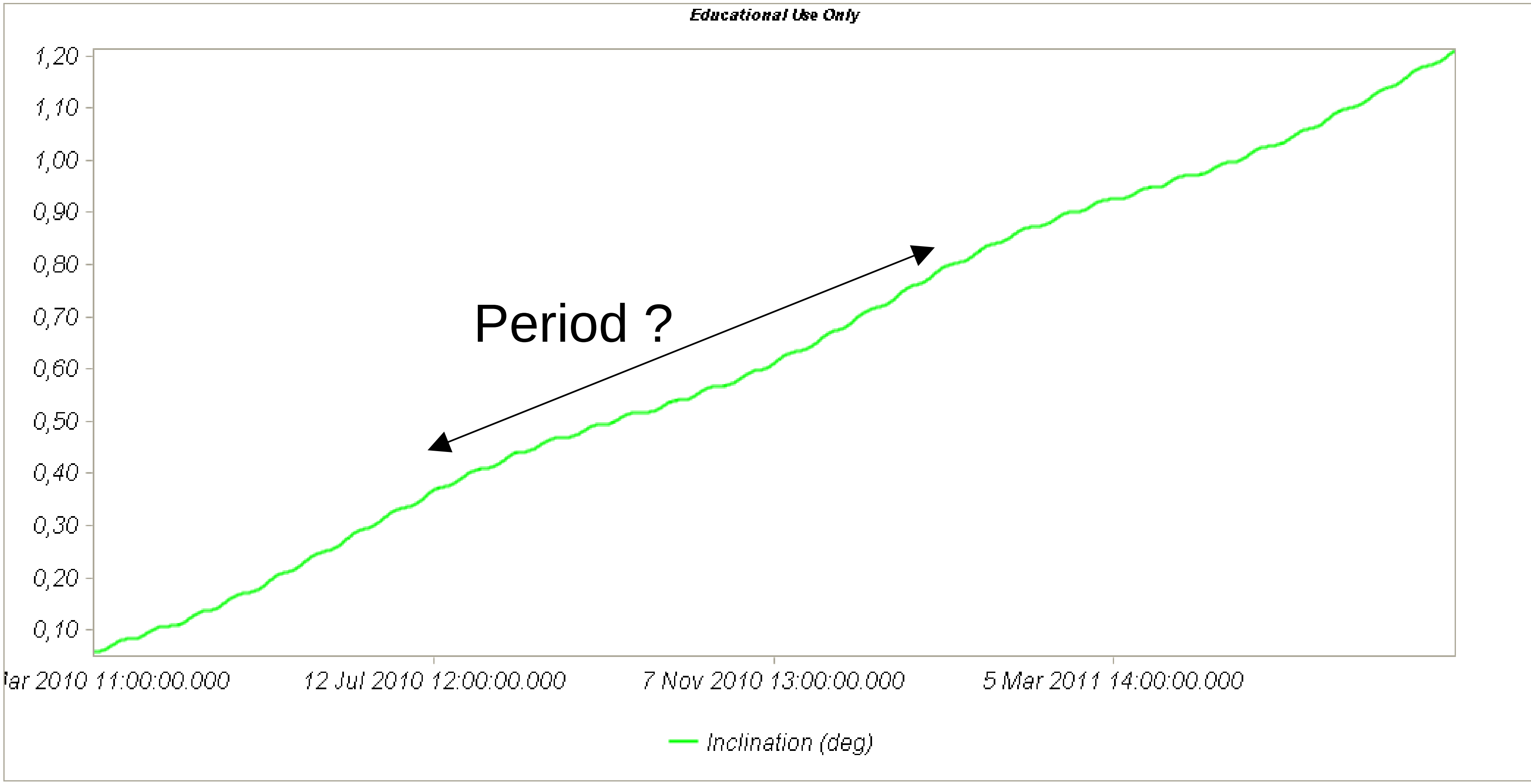

HPOP with Sun and Moon
(without oblateness/SRP/drag)

Thrust forces for stationkeeping

GEO spacecraft require continual stationkeeping to stay within the authorized box using onboard thrusters.

Mission orbit	Geostationary	(Allowable deviation from nominal position 0,1 deg)			
Launcher	Proton				
Launch in GTO					
Mission duration (yrs)	15				
Maneuvre	**delta v/maneuvre (m/s)**	**cycle time (days)**	**no. of maneuvers (-)**	**delta v/yr (m/s)**	**total delta V (m/s)**
Apogee kick	1836,49	*	1,0	*	1836,5
10 yr average NSSK	10,73	86,1	63,6	45,5	682,0
Worst Case NSSK	10,90	77,4	70,7	51,4	770,7
EWSK	0,13	35,3	155,3	1,33	19,9
Worst Case EWSK	NA	NA	NA	1,74	26,1
Orbit Maneuvres	0,00	*	0,0	*	0,0
Disposal	10,88	*	1,0	*	10,9
		Total Delta V (most favourable)			2549,3
		Total Delta V (worst case EWSK)			2555,5
		Total Delta V (worst case NSSK & EWSK)			2644,2

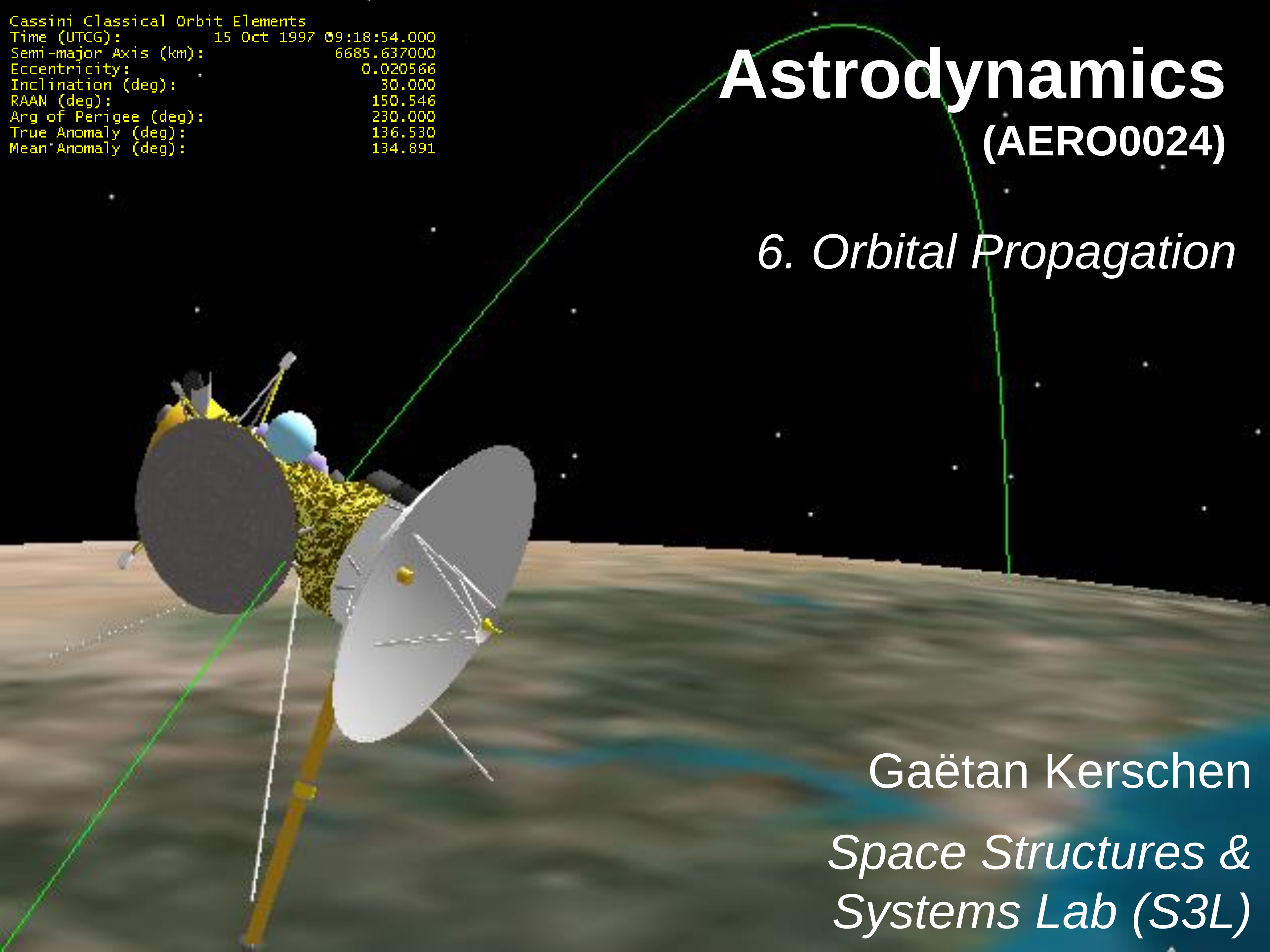

Astrodynamics
(AERO0024)

6. Orbital Propagation

Gaëtan Kerschen

Space Structures & Systems Lab (S3L)